

LECTURE 30:

Modeling Neuron-Glia Interactions 3

Marja-Leena Linne

Tampere University

Faculty of Medicine and Health Technology

Finland

marja-leena.linne@tuni.fi

LinkedIn: marjaleenalinne

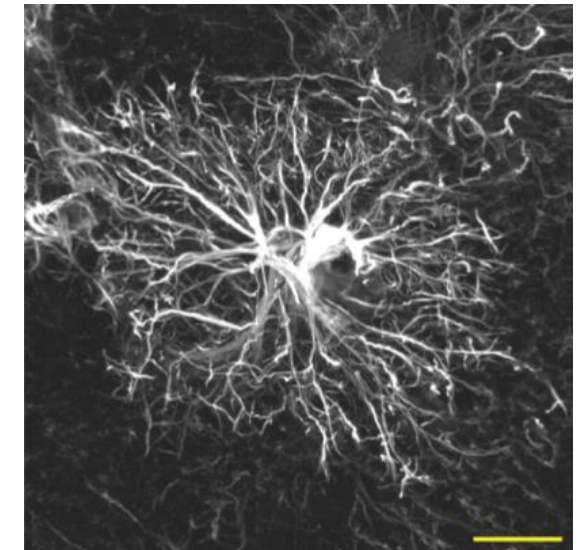
<https://research.tuni.fi/computational-neuroscience/>

LASCON X: Three lectures and one tutorial

1. Modeling Neuron-Glia Interactions 1: Biology of the Glial Cells & Background to Modeling
2. Modeling Neuron-Glia Interactions 2: Modeling Single Cells
3. **Modeling Neuron-Glia Interactions 3: Modeling Networks with Neuron-Glia Interactions**
4. Tutorial: NEST Astrocyte Modeling Tool

Contents

1. Summary of network models with neuron-glia interactions
2. Example: Neuron-astrocyte network model in NEST
3. Summary of tools for astrocyte modeling



Cortical astrocyte *in vivo*

1. Summary of network models with neuron-glia interactions

Computational network models with neuron-glia interactions

Neuroinformatics
<https://doi.org/10.1007/s12021-023-09622-w>

RESEARCH

Check for updates

Analysis of Network Models with Neuron-Astrocyte Interactions

Tiina Manninen¹ · Jugoslava Acimović¹ · Marja-Leena Linne¹ 

Accepted: 1 February 2023
© The Author(s) 2023

Abstract
Neural networks, composed of many neurons and governed by complex interactions between them, are a widely accepted formalism for modeling and exploring global dynamics and emergent properties in brain systems. In the past decades, experimental evidence of computationally relevant neuron-astrocyte interactions, as well as the astrocytic modulation of global neural dynamics, have accumulated. These findings motivated advances in computational glioscience and inspired several models integrating mechanisms of neuron-astrocyte interactions into the standard neural network formalism. These models were developed to study, for example, synchronization, information transfer, synaptic plasticity, and hyperexcitability, as well as classification tasks and hardware implementations. We here focus on network models of at least two neurons interacting bidirectionally with at least two astrocytes that include explicitly modeled astrocytic calcium dynamics. In this study, we analyze the evolution of these models and the biophysical, biochemical, cellular, and network mechanisms used to construct them. Based on our analysis, we propose how to systematically describe and categorize interaction schemes between cells in neuron-astrocyte networks. We additionally study the models in view of the existing experimental data and present future perspectives. Our analysis is an important first step towards understanding astrocytic contribution to brain functions. However, more advances are needed to collect comprehensive data about astrocyte morphology and physiology in vivo and to better integrate them in data-driven computational models. Broadening the discussion about theoretical approaches and expanding the computational tools is necessary to better understand astrocytes' roles in brain functions.

Keywords astrocyte · computational model · intracellular calcium · neuron-astrocyte network · simulation · synapse

Introduction

Modeling astrocytic functions, often together with neuronal or vascular functions, has been the trend in recent years, and, consequently, hundreds of computational models have been developed. Different aspects of these models have been reviewed before (see, e.g., Jolivet et al., 2010; Mangia et al., 2011; De Pittà et al., 2012, 2016; Fellin et al., 2012; Min et al., 2012; Volman et al., 2012; Wade et al., 2013; Linne & Jalonen, 2014; Tewari & Parpura, 2014; Manninen et al., 2018b, 2019; Denizot et al., 2020; González et al., 2020; Covelo et al., 2022; Linne et al., 2022). However, none of the previous surveys categorized and analyzed in detail all aspects of neuron-astrocyte network-level models. These aspects are: (1) bioelectricity in neurons, models for excitable neuronal membranes, (2) calcium (Ca^{2+}) and other cell biological mechanisms in astrocytes, (3) spatial organizations of cells, (4) structures of functional local interaction schemes between neurons and proximal astrocytes, (5) structures of global interaction schemes between each pair of modeled cell types (between neurons of different types), (6) directions of information flow, (7) inputs and outputs of the models (if any) including the stimulus protocols and the recorded variables, (8) origins and evolutions of the utilized models, (9) details of modeled neural systems (brain areas, developmental stages, etc.), and (10) availability of the model codes. To overcome this shortcoming, we decompose network models to their building blocks, systematically analyze and compare these blocks, and categorize the interactions between them. We also discuss what is missing in these computational models to explain different brain phenomena.

 Tiina Manninen
tiina.manninen@tuni.fi

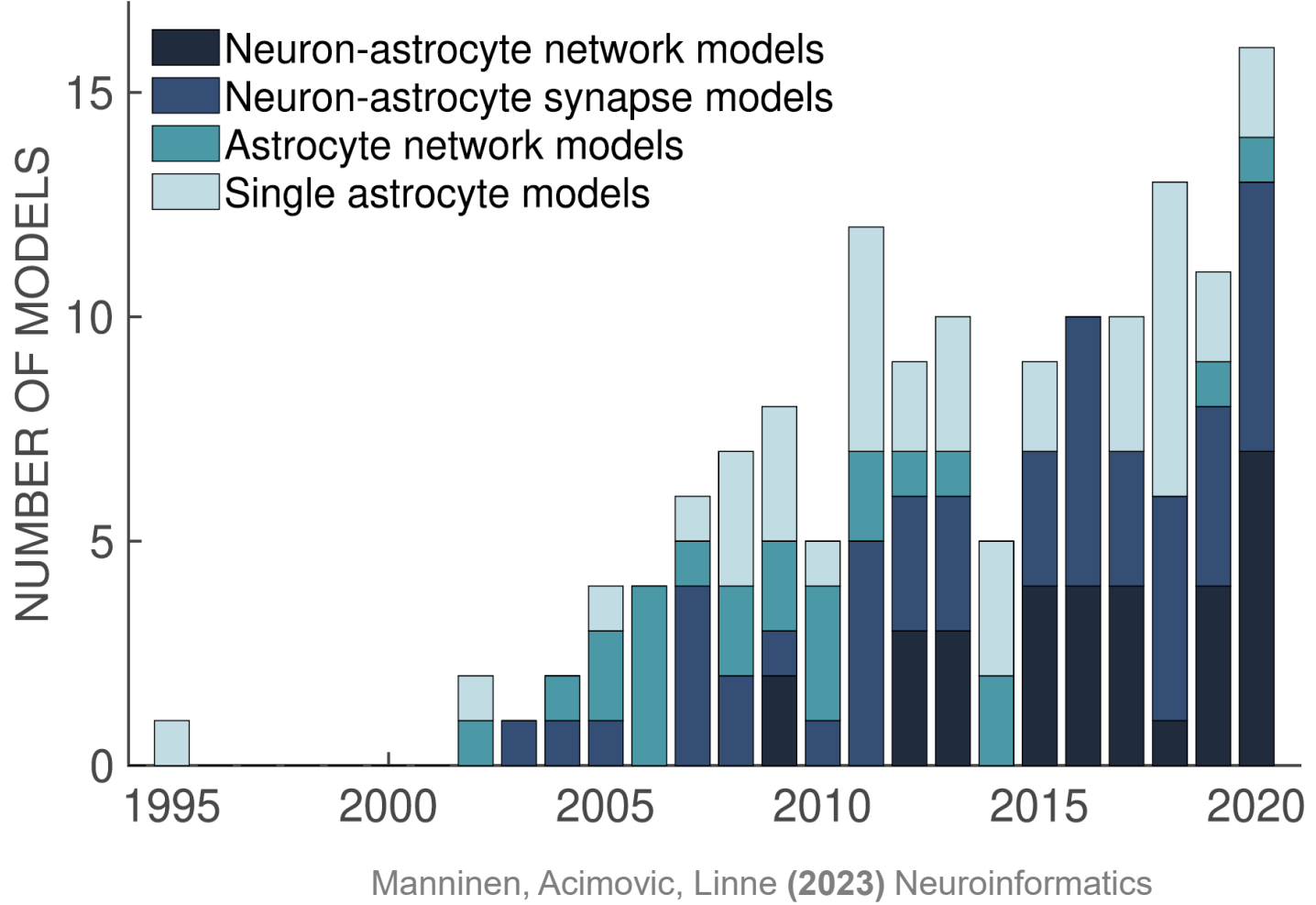
 Marja-Leena Linne
marja-leena.linne@tuni.fi

 Jugoslava Acimović
jugoslava.acimovic@tuni.fi

¹ Faculty of Medicine and Health Technology, Tampere University, Korkeakoulunkatu 3, FI-33720 Tampere, Finland

Published online: 23 March 2023

Springer



How did we select the models for analysis?



Model inclusion criteria:

- Astrocytic intracellular Ca^{2+} dynamics modeled with differential equations (time-, Ca^{2+} -, and at least one other astrocytic-variable dependent, e.g. IP_3).
- Astrocytic Ca^{2+} influences another signaling variable or intracellular astrocytic signal.
- Neuronal component includes at least one differential equation (e.g. membrane potential).
- Network structure includes ≥ 2 neurons and ≥ 2 astrocytes with bidirectional neuron–astrocyte interactions.

Outcome:

- Based on these criteria, **32 neuron–astrocyte network models** had been published by the end of 2020.

Model comparison framework

We systematically categorized and compared the 32 neuron–astrocyte network models across:

- Neuronal mechanisms
- Astrocytic mechanisms
- Functional neuron–astrocyte interactions (synaptic and non-synaptic)
- Structural organization of interactions among all modeled cell types



Characteristics of models for comparison

For each network model, we indicated the following:

- Brain area –specific or generic,
- Experimental data used for model construction and validation
- # of neurons of each type: excitatory neuron (E), inhibitory neuron (I), interneuron (IN), pyramidal neuron (PY), thalamocortical neuron (TC), and reticular thalamic neuron (RE)), # of astrocytes
- What kind of phenomena the network models explain:
 - Ca^{2+} dynamics (Ca^{2+})
 - excitatory-inhibitory balance (E-I balance)
 - synchronization (Sync.)
 - signal or information transfer (Sgn./Inf.)
 - synaptic plasticity (Plast.)
 - hyperexcitability (Hyper.)
- Engineering application: classification task (Classif.) or hardware (neuromorphic) implementation (HW)
- Programming language or simulation tool
- Model codes' availability in open-access online repositories.



Table 1 Characteristics of neuron-astrocyte network models. This table lists several details for each study: the tool or programming language used, code availability online, brain area, experimental data

Study	Tool/ availability	Brain ar
Abed et al. (2020)	n/a	Generic
Aleksin et al. (2017)	Arachne/GitHub	Hippocar
Allegri et al. (2009)	n/a	Cortex
Amiri et al. (2012a)	n/a	Hippocar
Amiri et al. (2012b)	Simulink®	Thalamo
Amiri et al. (2012c)	n/a	Thalamo
Amiri et al. (2013a)	Simulink®	Hippocar
Chan et al. (2017)	C++	Cortex/M
Gordleeva et al. (2019)	n/a	Hippocar
Haghiri et al. (2016)	HW	Generic
Haghiri et al. (2017)	HW	Generic
Haghiri and Ahmadi (2020)	n/a	Generic
Hayati et al. (2016)	HW	Generic
Kanakov et al. (2019)	n/a	Hippocar
Lenk et al. (2020)	INEXA	Generic
Li et al. (2016)	n/a	Hippocar
Li et al. (2020)	Brian 2	Cortex
Liu and Li (2013a)	n/a	Cortex
Liu and Li (2013b)	n/a	Generic
Liu et al. (2016)	HW	Generic
Makovkin et al. (2020)	n/a	Generic
Mesiti et al. (2015)	n/a	Hippocar
Naeem et al. (2015)	n/a	Generic
Nazari and Faez (2019)	n/a	Cortex
Nazari et al. (2020)	n/a	Cortex
Postnov et al. (2009)	n/a	Generic
Soleimani et al. (2015)	HW	Generic
Stimberg et al. (2019)	Brian 2/GitHub	Neocorte
Tang et al. (2017)	n/a	Cortex
Yang and Yeo (2015)	n/a	Spinal co
Yao et al. (2018)	n/a	Cortex
Yu et al. (2020)	n/a	Hippocar

ber of neurons and astrocytes, and experimentally shown neural function or other function that the model was finetuned to capture

Table 2 Characteristics of cellular interactions in the neuron-astrocyte network models. This table lists for each study, the number of connections and mechanisms in neuron-to-neuron (NN), neuron-to-astrocyte (NA), astrocyte-to-neuron (AN), and astrocyte-to-astrocyte (AA) interactions. Only those model details are shown that were clearly given in the model publications. Neurons are marked with N.

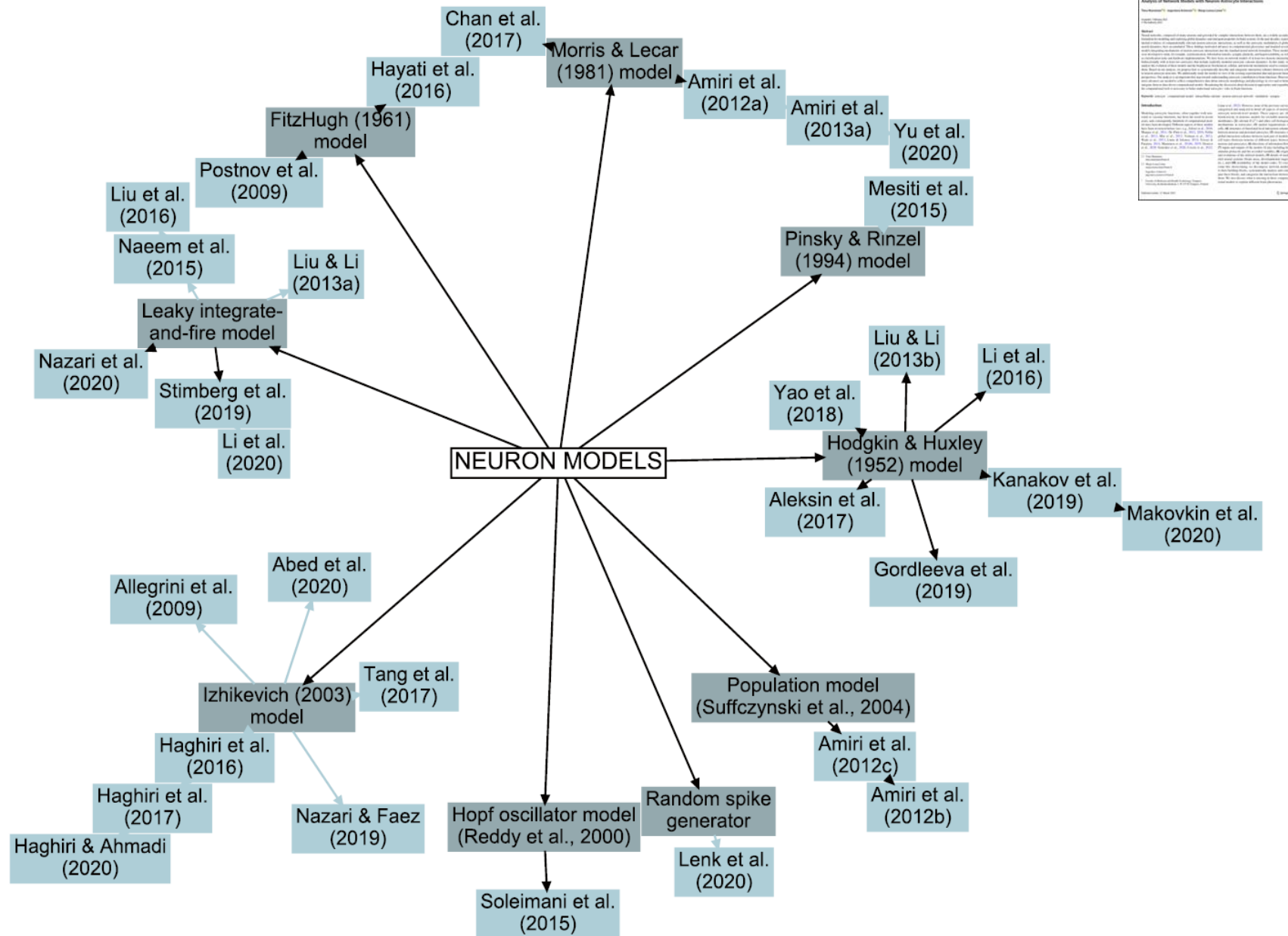
Study	NN interactions	NA interactions	AN interactions	AA interactions	
Li et al. (2016)	EE(100-1), EE(1, 100-2): $V_{\text{input}} \rightarrow \text{NT} \rightarrow s_{\text{syn}} \rightarrow I_{\text{syn}} \rightarrow V_{\text{input}}$	EA/A(1): $V_{\text{input}} \rightarrow \text{NT} \rightarrow [\text{IP}_3]_{\text{lat}}$	AE/A(1): $D_{\text{ext}} \cdot [\text{ATP}]_{\text{ext}} \cdot [\text{Glu}]_{\text{ext}} \cdot I_{\text{ext}, \text{ATP}} \rightarrow V_{\text{ext}, \text{PY}}$ $I_{\text{ext}, \text{Glu}} \rightarrow V_{\text{ext}, \text{PY}}, I_{\text{ext}, \text{ATP}} = c[\text{ATP}]_{\text{ext}}$ $I_{\text{ext}, \text{Glu}} = c[\text{Glu}]_{\text{ext}}$	AA(1-2): IP ₃ via GJs	
Li et al. (2020)	EE(100-100): $V_{\text{input}} \rightarrow p_{\text{synrel}} \rightarrow [\text{Glu}]_{\text{syn}} \rightarrow s_{\text{syn}, \text{AMPA/MEAR}} \rightarrow I_{\text{syn}, \text{AMPA/MEAR}} \rightarrow V_{\text{input}}$ $V_{\text{input}} \rightarrow p_{\text{synrel}} \rightarrow [\text{GABA}]_{\text{syn}} \rightarrow s_{\text{syn}, \text{GABAAR}} \rightarrow I_{\text{syn}, \text{GABAAR}} \rightarrow V_{\text{input}}$	EA(≈ 100): $V_{\text{input}} \rightarrow p_{\text{synrel}} \rightarrow [\text{Glu}]_{\text{syn}} \rightarrow [\text{IP}_3]_{\text{lat}}$	AE(≈ 100): $[\text{Ca}^{2+}]_{\text{ext}} \rightarrow p_{\text{ext}, \text{rel}} \rightarrow [\text{Glu}]_{\text{ext}} \rightarrow I_{\text{ext}, \text{Glu}} \rightarrow p_{\text{synrel}}$ $[\text{Ca}^{2+}]_{\text{ext}} \rightarrow p_{\text{ext}, \text{rel}} \rightarrow [\text{Glu}]_{\text{ext}} \rightarrow s_{\text{syn}, \text{AMPA/MEAR}} \rightarrow I_{\text{syn}, \text{AMPA/MEAR}} \rightarrow V_{\text{input}}$	AA(≈ 4): IP ₃ via GJs	
Study N					
Abed et al. (2020)	E				
Aleksin et al. (2017)	E				
Liu and Li (2013a)	Network 1: EE(100-10), EE(100-20); Network 2: EE(100): $V_{\text{input}} \rightarrow s_{\text{syn}} \rightarrow I_{\text{syn}} \rightarrow V_{\text{input}}$	Network 1 & 2: EA: $V_{\text{input}} \rightarrow [\text{Glu}]_{\text{syn}} \rightarrow [\text{IP}_3]_{\text{lat}}$	Network 1: AB(A1); Network 2: All: $I_{\text{ext}, \text{Glu}} \rightarrow V_{\text{ext}, \text{N}}$	Network 1 & 2: AA(2-4): Ca ²⁺ and IP ₃ via GJs	
Allegri et al. (2009)	E				
Liu and Li (2013b)	Network 1: EE(0-2); Network 2: EE(0-10-1), EE(1): Network 3: EE(0-1), EE(1); Network 4: EE(2), EE(0-1): $V_{\text{input}} \rightarrow p_{\text{synrel}} \rightarrow s_{\text{syn}} \rightarrow I_{\text{syn}} \rightarrow V_{\text{input}}$	Network 1, 2, 3 & 4: EA(1): $V_{\text{input}} \rightarrow [\text{IP}_3]_{\text{lat}}$	Network 1: AE(0-1); Network 2 & 3: AE/A(10-1); Network 4: AA(0-1): $I_{\text{ext}, \text{Glu}} \rightarrow V_{\text{ext}, \text{N}}$	Network 1, 2, 3 & 4: AA(2-3): Cu ²⁺ and IP ₃ via GJs	
Amiri et al. (2012a)	E				
Liu et al. (2016)	EE: $p_{\text{synrel}} \rightarrow I_{\text{syn}} \rightarrow V_{\text{input}}$ $V_{\text{input}} \rightarrow [2\text{-AG}]_{\text{post}} \rightarrow \text{DSE} \rightarrow p_{\text{synrel}}$	EA: $V_{\text{input}} \rightarrow [2\text{-AG}]_{\text{post}} \rightarrow [\text{IP}_3]_{\text{lat}}$	AE: $[\text{Ca}^{2+}]_{\text{ext}} \rightarrow [\text{Glu}]_{\text{ext}} \rightarrow e\text{-SP} \rightarrow p_{\text{synrel}}$	AA: IP ₃ via GJs	
Makovkin et al. (2020)	Network 1: EE(0-1); Network 2: EE(0-1): $V_{\text{input}} \rightarrow s_{\text{syn}} \rightarrow I_{\text{syn}} \rightarrow V_{\text{input}}$	Network 1: EA(1); Network 2: AA(1): $V_{\text{input/post}} \rightarrow \text{NT} \rightarrow [\text{IP}_3]_{\text{lat}}$	Network 1: AB(0-1); Network 2: AA(1): $[\text{Ca}^{2+}]_{\text{ext}} \rightarrow s_{\text{syn}} \rightarrow I_{\text{syn}} \rightarrow V_{\text{input}}$	Network 1 & 2: AA(1): Ca ²⁺ and IP ₃ via GJs	
Amiri et al. (2012b)	E				
Mesiti et al. (2015)	EE(0-1): $V_{\text{input, presyn}} \rightarrow s_{\text{syn}, \text{AMPA/MEAR}} \rightarrow I_{\text{syn}, \text{AMPA/MEAR}} \rightarrow V_{\text{input, post}}$	EA(0-1): $V_{\text{input, presyn}} \rightarrow [\text{IP}_3]_{\text{lat}}$	AB(0-2): $[\text{Ca}^{2+}]_{\text{ext}} \rightarrow [\text{Ca}^{2+}]_{\text{pre}}$ $[\text{Ca}^{2+}]_{\text{ext}} \rightarrow s_{\text{syn}, \text{AMPA/MEAR}} \rightarrow I_{\text{ext}, \text{AMPA/MEAR}} \rightarrow V_{\text{input, post}} \rightarrow I_{\text{ext}, \text{Glu}} \rightarrow V_{\text{input, presyn}}$	AA(1-2): IP ₃ via GJs	
Naeem et al. (2015)	n/a				
Nazari and Faez (2019)	n/a				
Nazari et al. (2020)	n/a				
Nazari and Faez (2019)	E	EE(0-1): $p_{\text{synrel}} \rightarrow I_{\text{syn}} \rightarrow V_{\text{input}}$ $V_{\text{input}} \rightarrow [2\text{-AG}]_{\text{post}} \rightarrow \text{DSE} \rightarrow p_{\text{synrel}}$	EA(0-1): $V_{\text{input}} \rightarrow [2\text{-AG}]_{\text{post}} \rightarrow [\text{IP}_3]_{\text{lat}}$	AB(1): $[\text{Ca}^{2+}]_{\text{ext}} \rightarrow [\text{Glu}]_{\text{ext}} \rightarrow e\text{-SP} \rightarrow p_{\text{synrel}}$	AA(2): IP ₃ via GJs
Liu and Li (2019)	E	EE/EV/EI(1/p = 0.08): $V_{\text{input}} \rightarrow s_{\text{AMPA/GABAAR}} \rightarrow I_{\text{syn}, \text{AMPA/GABAAR}} \rightarrow V_{\text{input}}$	EA/A(1): $V_{\text{input/post}} \rightarrow \text{NT} \rightarrow [\text{IP}_3]_{\text{lat}}$	AA(p = 0.1): IP ₃ via GJs	
Haghiri et al. (2016)	N	L2: EE/EV/EI(1/p = 0.2); From L2 to output layer: EE/EI(10): $V_{\text{input}} \rightarrow s_{\text{AMPA/GABAAR}} \rightarrow I_{\text{syn}, \text{AMPA/GABAAR}} \rightarrow V_{\text{input}}$	L2: EA/I(A0-1): $V_{\text{input/post}} \rightarrow \text{NT} \rightarrow [\text{IP}_3]_{\text{lat}}$	L2: AA(I, L673): IP ₃ via GJs	
Postnov et al. (2009)	N	EE(1): $V_{\text{input}} \rightarrow z \rightarrow I_{\text{syn}} \rightarrow w_{\text{post}}$	EA(I): $V_{\text{input}} \rightarrow z \rightarrow S_{\text{ext}}$ $w_{\text{post}} \rightarrow \text{Ca}_{\text{ext}}^{2+}$	AB: $G_{\text{ext}} \rightarrow I_{\text{ext}} \rightarrow w_{\text{post}}, I_{\text{ext}, \text{ATP}} \rightarrow w_{\text{post}}, I_{\text{ext}, \text{Glu}} \rightarrow G_{\text{ext}}$ $I_{\text{ext}} = (k - eG_{\text{ext}})(z - z_0)$	AA: Ca ²⁺ and IP ₃ via GJs, D _{ext} , ATP _{ext} , G _{ext} and Glu _{ext} , G _{ext}
Haghiri et al. (2017)	N				
Soleimani et al. (2015)	E	Network 1: EEC(4); Network 2: EI: $X_{\text{pre}} \rightarrow I_{\text{syn}} \rightarrow X_{\text{post}}$ $Y_{\text{pre}} \rightarrow I_{\text{syn}} \rightarrow Y_{\text{post}}$	Network 1 & 2: EA(2-4); Network 2: AA(1): $X_{\text{N}} \rightarrow Z \rightarrow S_{\text{ext}}, Y_{\text{N}} \rightarrow Z \rightarrow S_{\text{ext}}$	Network 1 & 2: AB(I): $I_{\text{ext}} \rightarrow X_{\text{N}}, I_{\text{ext}} \rightarrow Y_{\text{N}}$ $I_{\text{ext}} = c\text{Ca}^{2+}$	None
Stimberg et al. (2019)	E	EE/EI(1/p = 0.05), EI/EI(1/p = 0.2): $V_{\text{input}} \rightarrow p_{\text{synrel}} \rightarrow s_{\text{syn}} \rightarrow I_{\text{syn}} \rightarrow V_{\text{input}}$	EA(I): $V_{\text{input}} \rightarrow p_{\text{synrel}} \rightarrow [\text{NT}] \rightarrow I_{\text{ext}, \text{Glu}} \rightarrow [\text{IP}_3]_{\text{lat}}$	AB(I): $[\text{Ca}^{2+}]_{\text{ext}} \rightarrow p_{\text{ext}, \text{rel}} \rightarrow [\text{Gt}] \rightarrow s_{\text{pre}} \rightarrow p_{\text{synrel}}$	AA: IP ₃ via GJs
Tang et al. (2017)	E	EE(2-4): $V_{\text{input}} \rightarrow S \rightarrow V_{\text{input}}$	EA(I): $V_{\text{input}} \rightarrow [\text{IP}_3]_{\text{lat}}$	AB(I): $I_{\text{ext}, \text{Glu}} \rightarrow V_{\text{ext}, \text{N}}$	AA(1-2): IP ₃ via GJs
Yao et al. (2018)	E	EE: $[\text{Glu}]_{\text{syn}}$	EA: $[\text{Glu}]_{\text{syn}} \rightarrow [\text{IP}_3]_{\text{lat}}$	AB: $[\text{ATP}]_{\text{ext}} \rightarrow \text{NMDAR}_{\text{post}}, [\text{Glu}]_{\text{ext}} \rightarrow \text{NMDAR}_{\text{post}}$	AA: IP ₃ via GJs, D _{ext} , ATP _{ext} and Glu _{ext}
Yu et al. (2018)	E	EE(0-1): $[\text{K}^+]_{\text{ext}}, [\text{Na}^+]_{\text{ext}}$ $V_{\text{input}} \rightarrow [\text{Glu}]_{\text{ext}} \rightarrow I_{\text{syn}, \text{K/MEAR}} \rightarrow V_{\text{input}}$	EA(I): $[\text{K}^+]_{\text{ext}}, [\text{Na}^+]_{\text{ext}}$	AB(I): $[\text{K}^+]_{\text{ext}}, [\text{Na}^+]_{\text{ext}}$ $[\text{ATP}]_{\text{ext}} \rightarrow [\text{Glu}]_{\text{ext}} \rightarrow I_{\text{syn}, \text{K/MEAR}} \rightarrow V_{\text{input}}$	AA: $[\text{K}^+]_{\text{ext}}, [\text{Na}^+]_{\text{ext}}$ $[\text{ATP}]_{\text{ext}} \rightarrow [\text{Glu}]_{\text{ext}} \rightarrow [\text{Gt}]_{\text{ext}}, D_{\text{ext}}$ $[\text{ATP}]_{\text{ext}} \rightarrow [\text{Glu}]_{\text{ext}}, [\text{Na}^+]_{\text{ext}}$
Yu et al. (2020)	E	EE(100-1), EE(1, 100-2): $V_{\text{input}} \rightarrow \text{NT} \rightarrow s_{\text{syn}} \rightarrow I_{\text{syn}} \rightarrow V_{\text{input}}$	EA/A(50): $V_{\text{input}} \rightarrow \text{NT} \rightarrow [\text{IP}_3]_{\text{lat}}$ $A/A(50): I_{\text{ext}} \rightarrow V_{\text{ext}, \text{PY}}, I_{\text{ext}} = c \sum f$	AA(1-2): IP ₃ via GJs	

Origin of neuron models in network models



- Most studies used single-compartment models for both neurons and astrocytes.
- Some studies also employed multicompartment astrocyte models, with simple to detailed morphologies (Postnov et al., 2009; Liu & Li, 2013; Mesiti et al., 2015; Gordleeva et al., 2019).
- **Seven** studies utilized Hodgkin-Huxley models (Hodgkin & Huxley, 1952) and **one** utilized Pinsky-Rinzel model (Pinsky & Rinzel, 1994) derived from the model by Traub et al. (1991).
- **Four** studies used Morris-Lecar model (Morris & Lecar, 1981).
- **Two** studies used FitzHugh-Nagumo model (FitzHugh, 1961)
- **Six** studies used leaky integrate-and-fire (LIF) models, and
- **Seven** studies used Izhikevich model (Izhikevich, 2003).
- Among the modeled **ion channels** were T-type low-threshold Ca^{2+} (CaT) channels, transient K^+ (KA) channels, Ca^{2+} -activated K^+ (KCa) channels, delayed rectifier K^+ (KDR) channels, afterhyperpolarization (AHP) channels, persistent Na^+ (NaP) channels, and fast transient Na^+ (NaT) channels.

Evolution of neuron models in the neuron-astrocyte network models

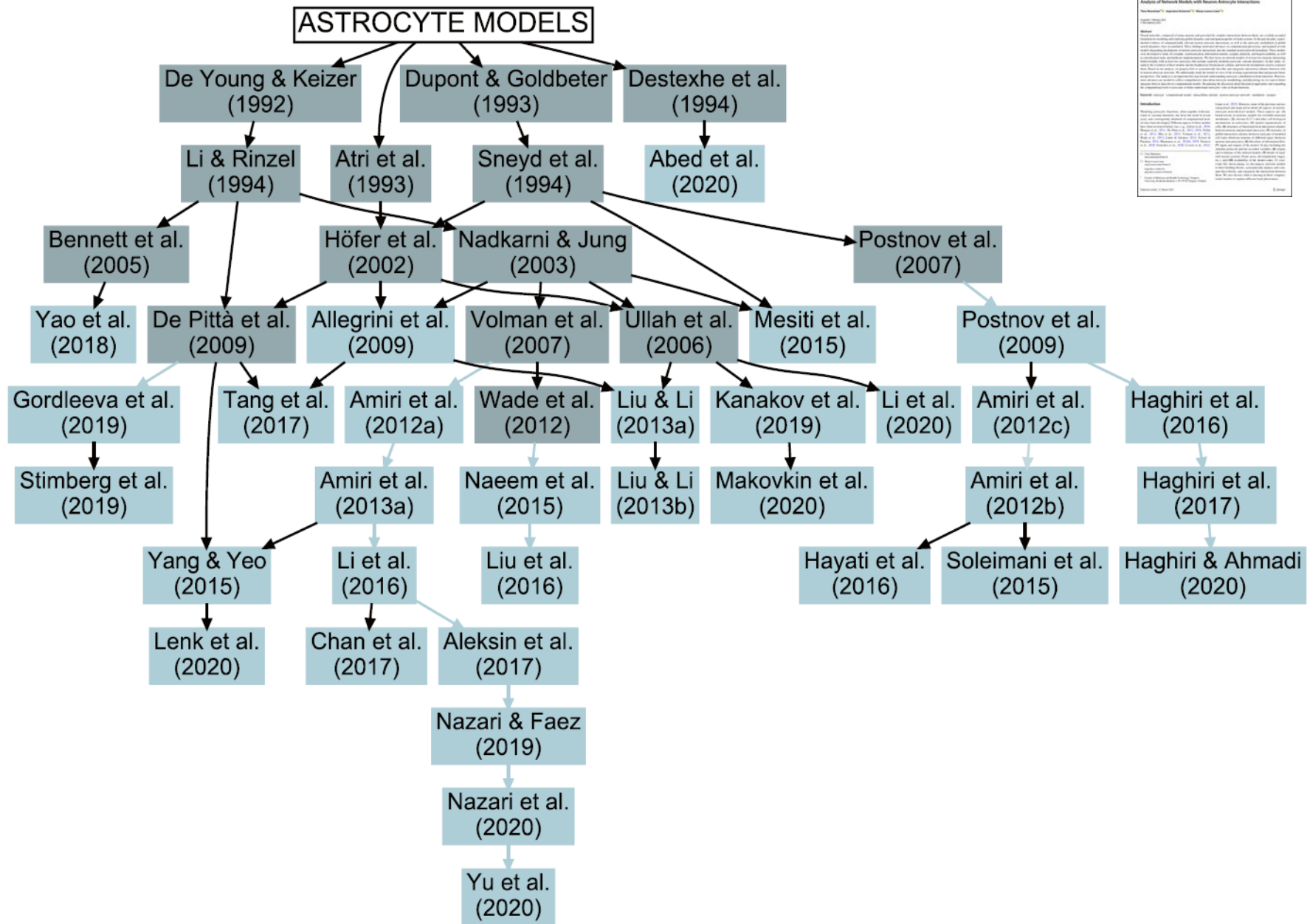


Origin of astrocyte models in network models

- Most of the astrocyte models resemble closely the Ca^{2+} dynamics models originally developed for other cells, such as neurons, oocytes, or epithelial cells:
 - De Young & Keizer, 1992; Atri et al., 1993; Dupont & Goldbeter, 1993; Destexhe et al., 1994; Li & Rinzel, 1994; Sneyd et al., 1994.
- In addition, the astrocyte models by Höfer et al. (2002), Nadkarni and Jung (2003), Bennett et al. (2005), Ullah et al. (2006), Postnov et al. (2007), Volman et al. (2007), De Pittà et al. (2009), and Wade et al. (2012) built based on the above models, were used when building the network models.
- All these models initially originate from the **CICR model by Bezprozvanny et al. (1991)**.
- Thus, in the end, almost all astrocytic Ca^{2+} dynamics models have evolved from the **very early models of calcium dynamics originally developed for other cell types than the astrocytes**.



Evolution of astrocyte models in the neuron-astrocyte network models

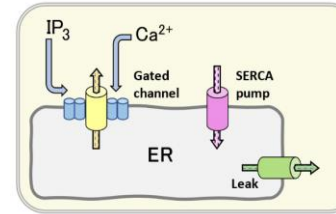


Details of astrocyte descriptions in network models

- The astrocytic Ca^{2+} dynamics models mostly had the same general mathematical structure.

- Typical model components:

- IP3Rs (CICR),
- SERCA pumps, and
- the leak flux from the ER to the cytosol.



- Examples of the additional plasma membrane mechanisms are:

- PMCA pumps (Yao et al., 2018),
- Capacitive Ca^{2+} entry (CCE) (Kanakov et al., 2019; Makovkin et al., 2020), and
- K^+ and Na^+ channels (Yao et al., 2018).

- About half of the models had influx of Ca^{2+} from extracellular space or efflux of Ca^{2+} to extracellular space.
- Intracellular diffusion of Ca^{2+} and IP_3 was included in six models (Allegrini et al., 2009; Postnov et al., 2009; Liu & Li, 2013a, b; Mesiti et al., 2015; Gordleeva et al., 2019).
- Gliotransmitters were included as astrocytic variables when modeled by differential equations and were often used as inputs to activate other cells.

Characteristics of cellular interactions in network models



Study	NN interactions	NA interactions	AN interactions	AA interactions
Abed et al. (2020)	EE/EI/IE/II: $V_{m,pre} \rightarrow S \rightarrow V_{m,post}$	EA/IA: $V_{m,pre} \rightarrow NT \rightarrow IP_3_{ast}$	AE/AI: $I_{ast} \rightarrow V_{m,post}, I_{ast} = cGlu_{ext}$	AA: IP_3 via GJs
Aleksin et al. (2017)	EE/II(2), EI/IE(0-1): $V_{m,pre} \rightarrow g_{syn} \rightarrow I_{syn} \rightarrow V_{m,post}$	EA/IA(0-1): $V_{m,pre} \rightarrow [NT] \rightarrow [IP_3]_{ast}$	AE/AI(0-1): $[Ca^{2+}]_{ast} \rightarrow p_{syn,rel}$	AA(2): Ca^{2+} via GJs
Allegrini et al. (2009)	EE/EI/IE/II: $V_{m,pre} \rightarrow S \rightarrow V_{m,post}$	EA(1): $V_{m,pre} \rightarrow [IP_3]_{ast}$	AE/AI: $I_{astro} \rightarrow V_{m,post}$	AA(2-4): Ca^{2+} and IP_3 via GJs
Amiri et al. (2012a)	EE/II(0-1), EI(1), IE(1-2): $V_{m,pre} \rightarrow NT \rightarrow g_{syn} \rightarrow I_{syn} \rightarrow V_{m,post}$	EA(1): $V_{m,pre} \rightarrow NT \rightarrow [IP_3]_{ast}$	AE/AI(1): $I_{ast} \rightarrow V_{m,PY/IN}, I_{ast} = cf$	AA(1-2): IP_3 via GJs
Amiri et al. (2012b)	EE/EI/IE: $V_{m,pre} \rightarrow g_{syn,AMPAR/GABAAR/GABABR} \rightarrow I_{syn,AMPAR/GABAAR/GABABR} \rightarrow V_{m,post}, C_{gain}$	EA: $F_{PY} \rightarrow S_m$	AE/AI: $G_m \rightarrow C_{gain}$	AA: IP_3 via GJs
Amiri et al. (2012c)	EE/EI/IE: $V_{m,pre} \rightarrow g_{syn,AMPAR/GABAAR/GABABR} \rightarrow I_{syn,AMPAR/GABAAR/GABABR} \rightarrow V_{m,post}, C_{gain}$	EA: $F_{PY} \rightarrow S_m$	AE/AI: $G_m \rightarrow C_{gain}$	AA: IP_3 via GJs
Amiri et al. (2013a)	EE/II(0-1), EI(1), IE(1-2): $V_{m,pre} \rightarrow NT \rightarrow g_{syn} \rightarrow I_{syn} \rightarrow V_{m,post}$	EA/IA(1): $V_{m,pre} \rightarrow NT \rightarrow [IP_3]_{ast}$	AE/AI(1): $I_{ast} \rightarrow V_{m,PY/IN}, I_{ast} = cf$	AA(1-2): IP_3 via GJs
Chan et al. (2017)	Network 1 & 2: EE($p = 0.19$), EI($p = 0.23$), IE($p = 0.21$), II($p = 0.17$): $V_{m,pre} \rightarrow g_{syn} \rightarrow I_{syn} \rightarrow V_{m,post}$	Network 1 & 2: EA/IA: $V_{m,N} \rightarrow [IP_3]_{ast}$	Network 1 & 2: AE/AI: $I_{ast} \rightarrow V_{m,E/I}, I_{ast} = cf$	Network 2: AA: IP_3 via GJs
Gordleeva et al. (2019)	EE($p = 0.2$): $V_{m,pre} \rightarrow Glu_{syn} \rightarrow I_{syn,NMDAR} \rightarrow V_{m,post}$	EA(1-2): $V_{m,pre} \rightarrow Glu_{syn} \rightarrow [IP_3]_{ast}$	AE(1, 14, 28): $[Ca^{2+}]_{ast} \rightarrow D\text{-serine}_{ext} \rightarrow I_{syn,NMDAR} \rightarrow V_{m,post}$ $[Ca^{2+}]_{ast} \rightarrow Glu_{ext} \rightarrow Glu_{syn} \rightarrow I_{syn,NMDAR} \rightarrow V_{m,post}$	AA(1): Ca^{2+} and IP_3 via GJs
Haghiri et al. (2016)	Network 1 & 2: EE(0-1): $V_{m,pre} \rightarrow z \rightarrow I_{syn} \rightarrow V_{m,post}$	Network 1: EA(1-4); Network 2: EA(1-2): $u_{post} \rightarrow Ca^{2+}_{ast}$ $V_{m,pre} \rightarrow z \rightarrow S_m$	Network 1 & 2: AE(1): $G_m \rightarrow I_{syn} \rightarrow V_{m,post}$ $I_{ast} \rightarrow V_{m,post}, I_{ast} = cG_m, I_{syn} = (k - cG_m)(z - z_0)$	Network 2: AA(1-2): n/a
Haghiri et al. (2017)	Network 1: EE(0-1); Network 2: EE: $V_{m,pre} \rightarrow z \rightarrow I_{syn} \rightarrow V_{m,post}$	Network 1: EA(1-2); Network 2: EA(0-2): $u_{post} \rightarrow Ca^{2+}_{ast}$ $V_{m,pre} \rightarrow z \rightarrow S_m$	Network 1 & 2: AE(1): $G_m \rightarrow I_{syn} \rightarrow V_{m,post}$ $I_{ast,ATP/Glu} \rightarrow V_{m,post}, I_{ast,ATP} = cG_a, I_{ast,Glu} = cG_m, I_{syn} = (k - cG_m)(z - z_0)$	None
Haghiri and Ahmadi (2020)	EE: $V_{m,pre} \rightarrow z \rightarrow I_{syn} \rightarrow V_{m,post}$	EA(1): $u_{post} \rightarrow Ca^{2+}_{ast}$ $V_{m,pre} \rightarrow z \rightarrow S_m$	AE(1): $G_m \rightarrow I_{syn} \rightarrow V_{m,post}, I_{ast} \rightarrow V_{m,post}, I_{ast} = cG_m, I_{syn} = (k - cG_m)(z - z_0)$	None
Hayati et al. (2016)	EE(0-1): $V_{m,pre} \rightarrow z \rightarrow I_{syn} \rightarrow V_{m,post}$	EA(1-4): $V_{m,pre} \rightarrow z \rightarrow S_m$, $w_{post} \rightarrow Ca^{2+}_{ast}$	AE(2): $G_m \rightarrow I_{syn} \rightarrow V_{m,post}, I_{ast} \rightarrow V_{m,post}, I_{ast} = cG_m, I_{syn} = (k - cG_m)(z - z_0)$	AA: n/a
Kanakov et al. (2019)	Network 1: EE/EI/IE($p = 0.33$); Network 2: EE(5): $V_{m,pre} \rightarrow g_{syn} \rightarrow I_{syn} \rightarrow V_{m,post}$	Network 1: EA/IA(1); Network 2: EA(1): n/a	Network 1: AE/AI(1); Network 2: AE(1): $[Ca^{2+}]_{ast} \rightarrow g_{syn} \rightarrow I_{syn} \rightarrow V_{m,post}$	Network 1 & 2: AA(2-3): Ca^{2+} and IP_3 via GJs
Lenket al. (2020)	EE/EI/IE/II($p = 0.29$): $F_{pre} \rightarrow p_{spike} \rightarrow p_{syn,rel} \rightarrow NT \rightarrow I_{syn} \rightarrow F_{post}$	EA(0-1): $F_{pre} \rightarrow p_{spike} \rightarrow p_{syn,rel} \rightarrow NT \rightarrow [IP_3]_{ast}$	AE/AI(130-250): $[Ca^{2+}]_{ast} \rightarrow S_{R,pre} \rightarrow p_{syn,rel}, S_{ast} \rightarrow F_{post}$	AA(1-5): IP_3 via GJs

Brain area and use of experimental data



- 12 models were **generic** models not developed for any specific brain area.
- Nine models were specialized to **cerebral cortex**, eight to **hippocampus**, one to **spinal cord**, and two to **thalamocortical** networks.
- Only **two** of the studies compared the simulation results **to experimental data** either qualitatively or quantitatively (Amiri et al., 2013a; Chan et al., 2017).
 - Amiri et al. (2013a) compared their model to local field potential (LFP) recordings from rat hippocampal (CA1) brain slices *in vitro*.
 - Chan et al. (2017) compared their model to multi-electrode array (MEA) recordings from dissociated cortical cultures of Wistar rat embryos at day 18.

Programming language or tool

- Out of the 32 models, **seven** named the simulation tool or programming language used.
- Out of the 32 models, only for **two** of the models the model codes were available online (**Aleksin et al., 2017; Stimberg et al., 2019**).
 - Aleksin et al. (2017) developed and used **Arachne** (C++, MATLAB®) to implement their model and made their model code available both as a supplementary to their article and in GitHub (<https://github.com/LeonidSavtchenko/Arachne/tree/master/ExamplePLOS>).
 - Stimberg et al. (2019) implemented their model with **Brian 2** (Goodman & Brette, 2008) and made their model code available in GitHub (<https://github.com/mdepitta/comp-glia-book/tree/master/Ch18.Stimberg>).

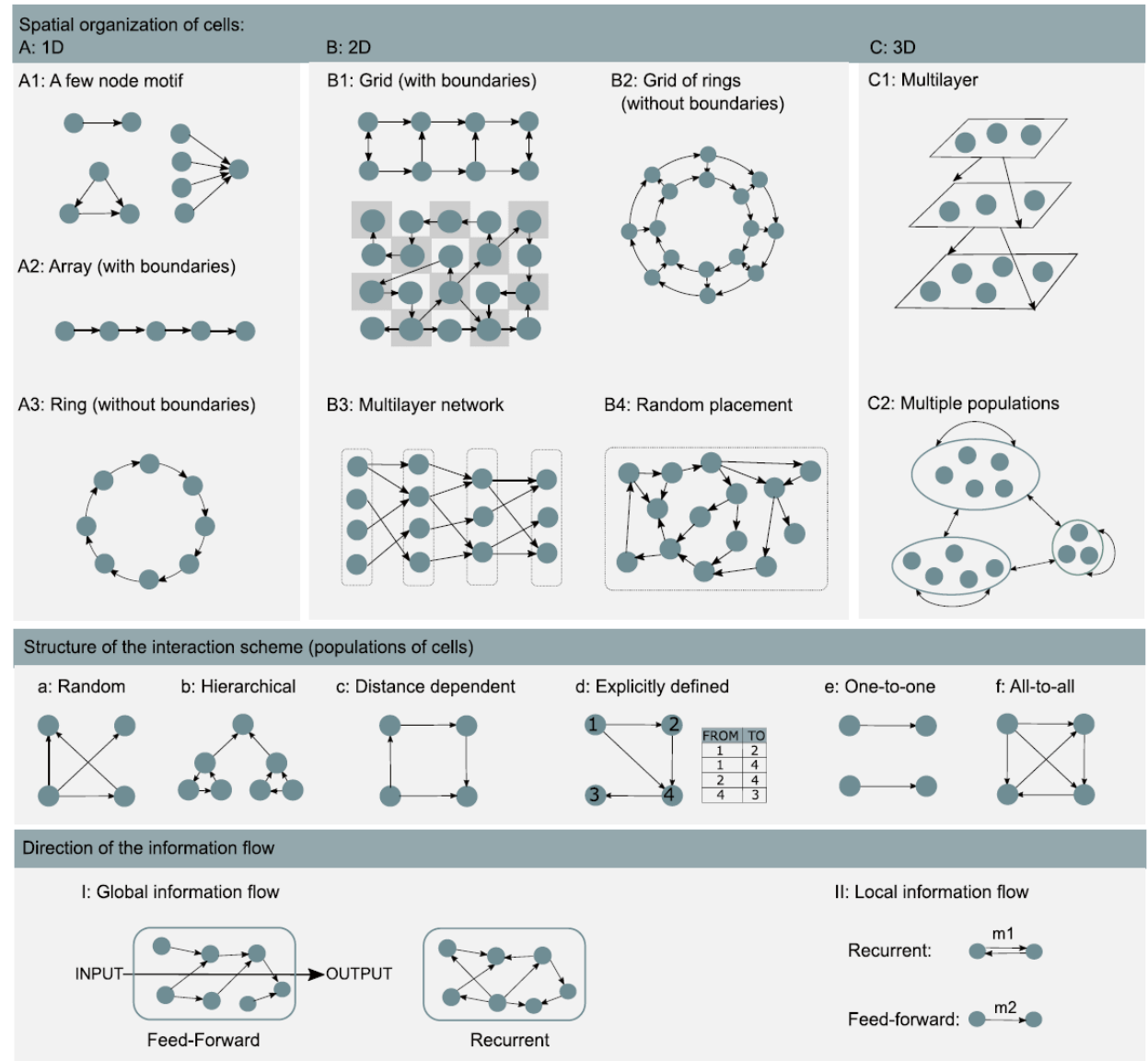


Spatial organization and structure of interactions between cells

- Spatial organization of cells
- Structure of the interaction scheme
- Direction of information flow

See also more detailed tables in the publication.

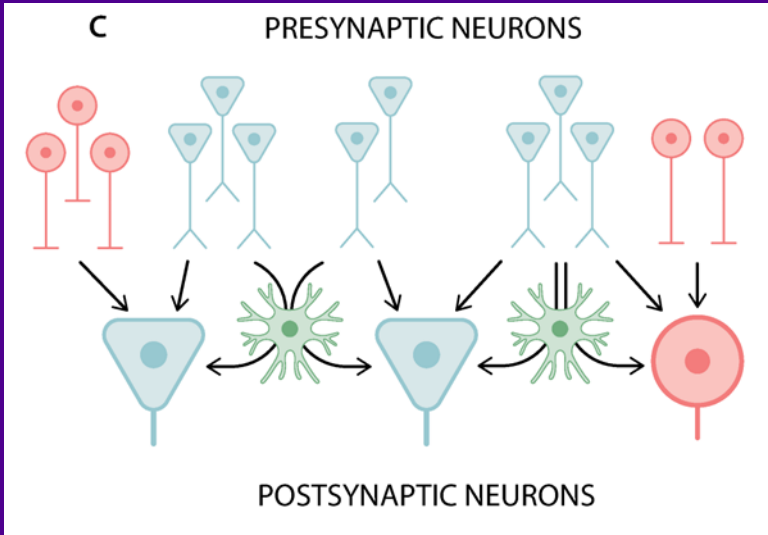
Manninen, Acimovic, Linne (2023) Neuroinformatics



2.1. Example:

Neuron-astrocyte network model in NEST

Network modeling with neuron-astrocyte interactions



nest::

PLOS COMPUTATIONAL BIOLOGY

RESEARCH ARTICLE

Modeling neuron-astrocyte interactions in neural networks using distributed simulation

Han-Jia Jiang ^{1,2*}, Jugoslava Acimović ^{3†}, Tiina Manninen ³, Iiro Ahokainen ³, Jonas Stappmanns ^{1,4}, Mikko Lehtimäki ³, Markus Diesmann ^{1,4,5}, Sacha J. van Albada ^{1,2}, Hans Ekkehard Plessner ^{1,6,7†}, Marja-Leena Linne ^{3,8†}

¹ Institute for Advanced Simulation (IAS-6), Jülich Research Centre, Jülich, Germany, ² Institute of Zoology, Faculty of Mathematics and Natural Sciences, University of Cologne, Cologne, Germany, ³ Faculty of Medicine and Health Technology, Tampere University, Tampere, Finland, ⁴ Department of Physics, Faculty 1, RWTH Aachen University, Aachen, Germany, ⁵ Department of Psychiatry, Psychotherapy and Psychosomatics, School of Medicine, RWTH Aachen University, Aachen, Germany, ⁶ Department of Data Science, Faculty of Science and Technology, Norwegian University of Life Sciences, Ås, Norway, ⁷ Käte Hamburger Kolleg: Cultures of Research (co:re), RWTH Aachen University, Aachen, Germany

* These authors contributed equally to this work.

† hijiang2@mail.uni-koeln.de (H-JJ), jugoslava.acimovic@tuni.fi (JA), marja-leena.linne@tuni.fi (M-LL)

Check for updates

OPEN ACCESS

Citation: Jiang H-J, Acimović J, Manninen T, Ahokainen I, Stappmanns J, Lehtimäki M, et al. (2025) Modeling neuron-astrocyte interactions in neural networks using distributed simulation. PLoS Comput Biol 21(9): e1013503. <https://doi.org/10.1371/journal.pcbi.1013503>

Editor: Joanna Jędrzejewska-Szmeik, Instytut Dydaktyki Doswiadczonej im M Nenckiego Polskiej Akademii Nauk, POLAND

Received: November 12, 2024

Accepted: September 8, 2025

Published: September 19, 2025

Copyright: © 2025 Jiang et al. This is an open access article distributed under the terms of the Creative Commons Attribution License, which permits unrestricted use, distribution, and reproduction in any medium, provided the original author and source are credited.

Data availability statement: The implemented astrocyte support is described in the user-level documentation of the latest release of NEST simulation code. Benchmark code and the code for developing and simulating the *in silico* model are available at <https://doi.org/10.5281/zenodo.13757202>. The supporting information (S1 Appendix, S2 Appendix, S3 Appendix, S4 Appendix) describe the specification of the network models used in this study, new variables and parameters of



Markus
Diesmann



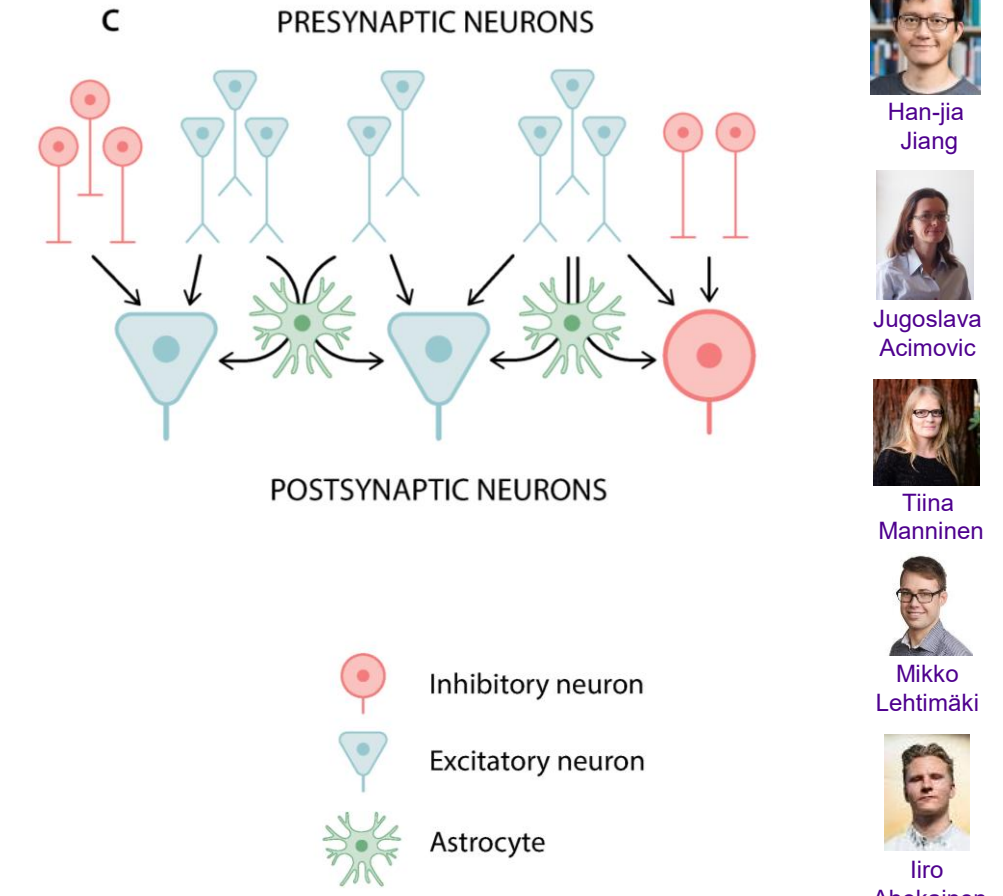
Sacha
Van Albada



Hans Ekkehard
Blesser

Goals

- Engineering goal:
Develop a simulation tool for modeling neuron–astrocyte interactions in large-scale brain networks.
- Scientific research question:
Can local astrocytic modulation of synaptic transmission synchronize global brain network activity (beyond the reach of current experimental methods)?



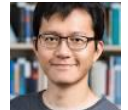
Markus
Diesmann



Sacha
Van Albada



Hans Ekkehard
Blesser



Han-jia
Jiang



Jugoslava
Acimovic



Tiina
Manninen



Mikko
Lehtimäki

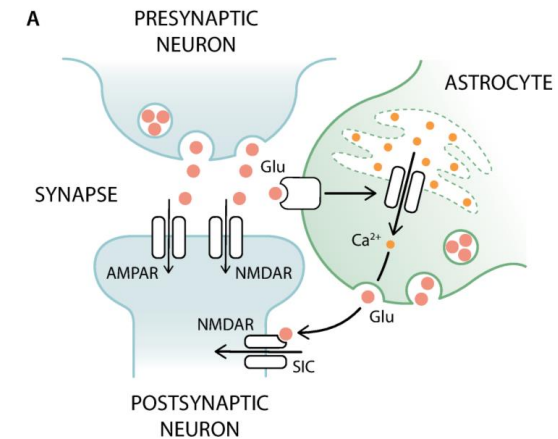


Iiro
Ahokainen

Methods

- **Connectivity model:** Tripartite connection rule extending the standard notion of binary connectivity between neurons
- **Astrocyte model:** Astrocytic calcium dynamics (ER, IP3R, SERCA pump, leak current)
- **Neuron model:** extended AdEx
- **Models for astrocyte-neuron interactions:**
 - mGluR sensing of synaptic glutamate
 - slow inward current (SIC) activated by calcium-dependent glutamate release from astrocytes
- Implementation in NEST simulator 3.6/3.8
- Simulation on 128-core compute nodes of Supercomputer JURECA at Juelich Research Centre

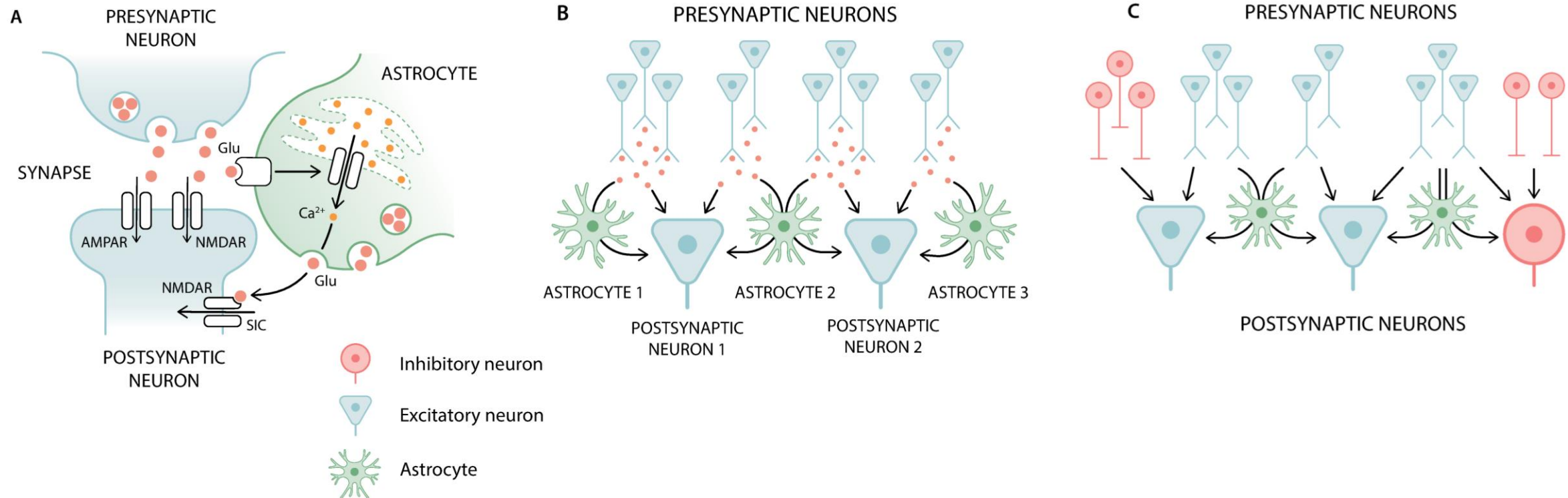
TRIPARTITE SYNAPSE



nest::



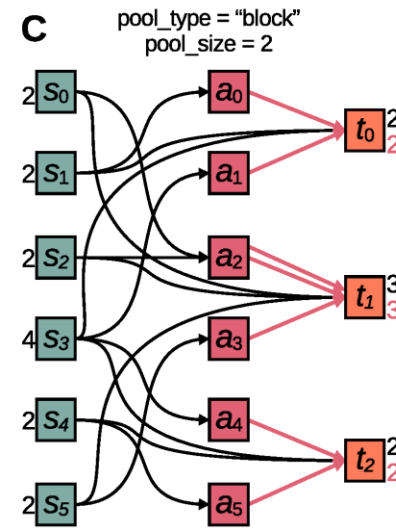
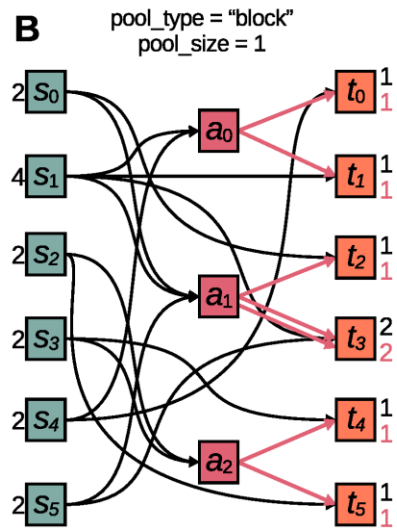
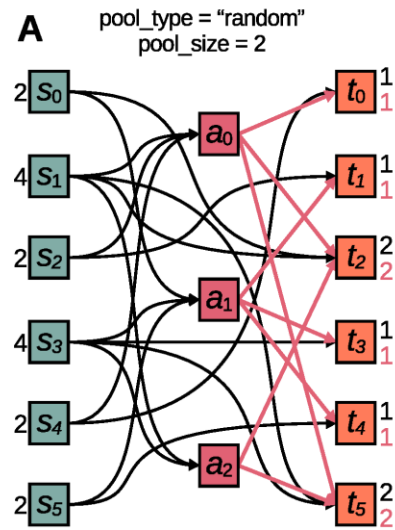
Result 1: New model-building framework for biophysical modeling of neurons and astrocytes in brain networks



Jiang, J. Aćimović, T. Manninen, I. Ahokainen, J. Stapmanns, M. Lehtimäki, M. Diesmann, S.J. van Albada, H.E. Plesser, M.-L. Linne. (2025) Modeling neuron-astrocyte interactions in neural networks using distributed simulation. PLoS Computational Biology.

Result 2: Novel tripartite connectivity specification

Primary connection rule; Third-factor connection rule



Example of NEST code to set up tripartite connectivity:

```
astrocytes = nest.Create(  
    "astrocyte_lr_1994", 100, {"Ca_tot": 2.0, "IP3_0": 0.16})  
  
neurons = nest.Create(  
    "aeif_cond_alpha_astro", 100, {"E_L": -70.6, "V_th": -50.4})  
  
nest.TripartiteConnect(  
    neurons, neurons, astrocytes,  
    conn_spec={"rule": "pairwise_bernoulli", "p": 0.1},  
    third_factor_conn_spec={  
        "rule": "third_factor_bernoulli_with_pool",  
        "p": 0.5,  
        "pool_size": 10,  
        "pool_type": "random"},  
    syn_specs={  
        "primary": {"synapse_model": "tsodyks_synapse", "weight": 0.7}  
        "third_in": {"synapse_model": "tsodyks_synapse", "weight": 0.3}  
        "third_out": {"synapse_model": "sic_connection", "weight": 1.0}})
```

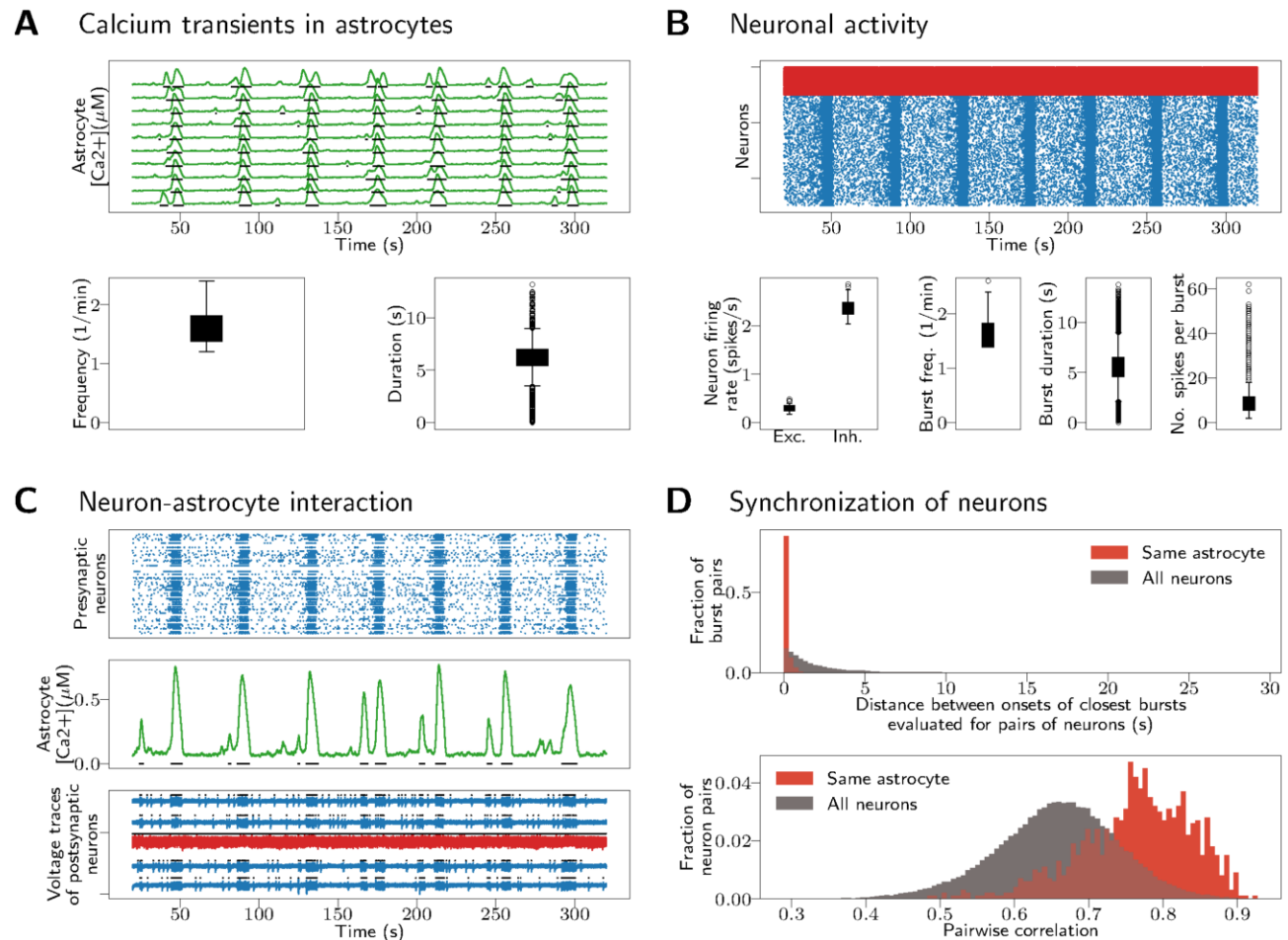
A) Random connectivity (arbitrary pool size, Spool).

B) Each target neuron t can interact with one astrocyte (Spool = 1).

C) Each target neuron t can interact with up to n astrocytes (here Spool = 2).

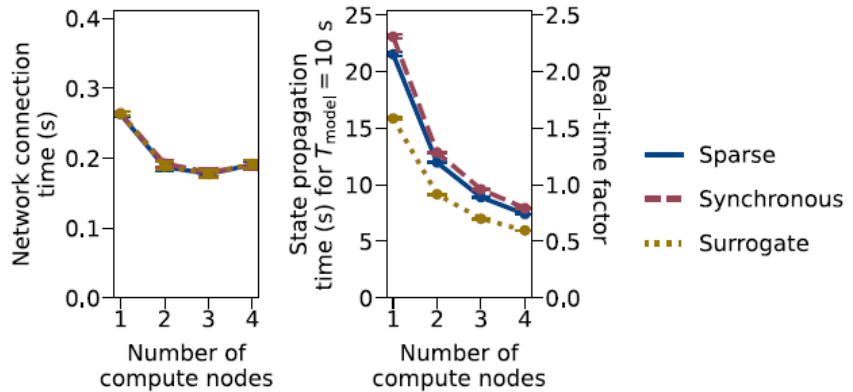
Result 3: Synchronization in neuron-astrocyte networks

- Maximal number of astrocytes interacting with a target neuron is 1 (Spool = 1).
- Increasing the input to an astrocyte results in the emergence of network-wide bursts lasting an average of 5 s.
- Experimental evidence from slice studies supporting our findings (Pirttimäki et al. 2012).

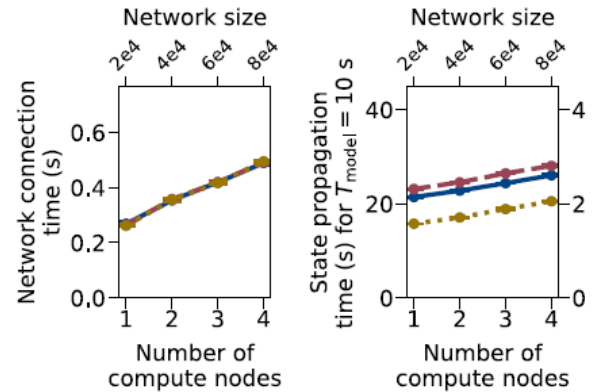


Result 4: Benchmarking the simulation technology using up to 1 million cells

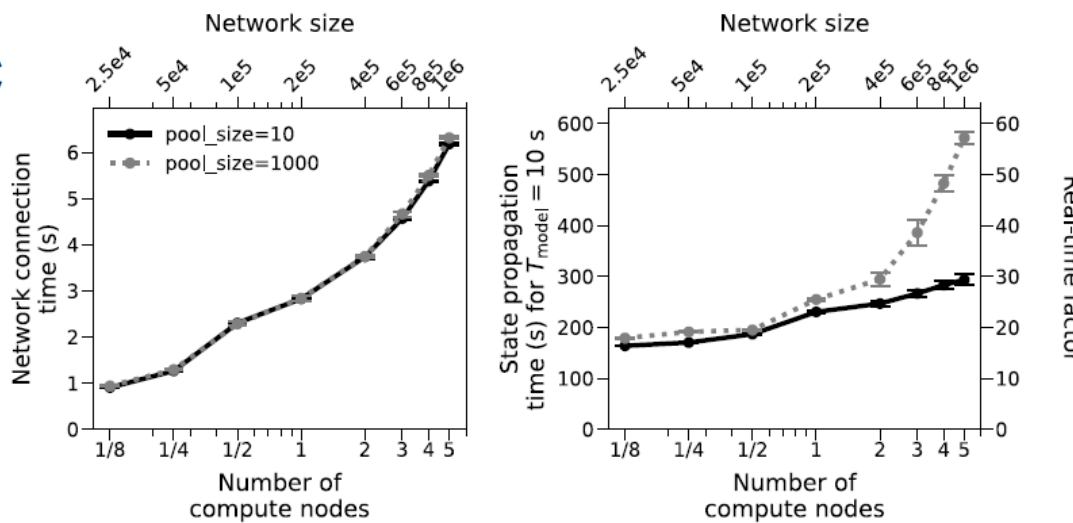
A Strong scaling



B Weak scaling



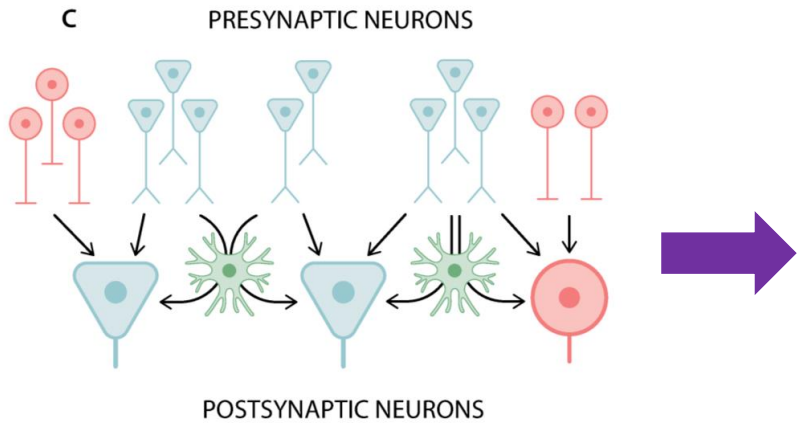
C



Strong scaling shows how fast a solution can be achieved if more resources (=compute nodes) are invested.

Weak scaling shows how time to solution changes if resources are increased proportional to scale of the model (=number of cells).

Future Outlook: Investigating neuron–astrocyte interactions in large-scale cortical networks *in vivo* and *in vitro*

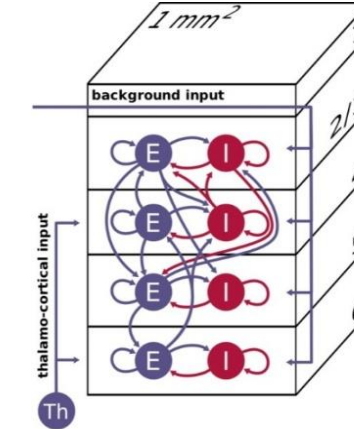


Jiang et al. (2025) PLoS Computational Biology

nest::
simulated()

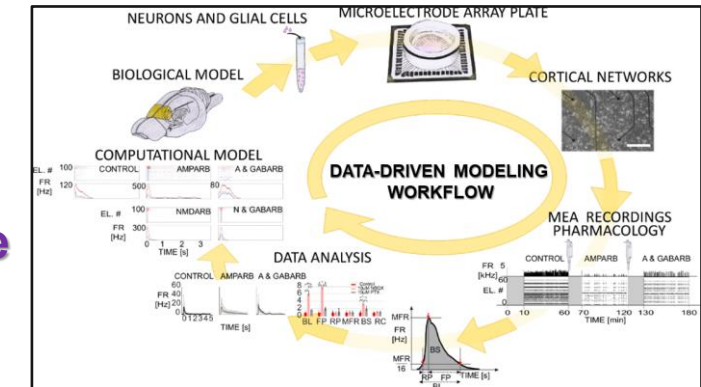
```
Calcium current input
-----
In this implementation, a current input to the astrocyte is directly
added to its cytosolic calcium concentration. Generators that send out currents
can be connected to astrocytes to directly generate fluctuations in cytosolic
calcium:
.. math:
\frac{d[\mathit{Ca}^{(2+)}]}{dt} = J_{\text{channel}} - J_{\text{pump}} + J_{\text{leak}} + J_{\text{noise}}
Here,  $J_{\text{channel}}$  is the cytosolic calcium concentration, and
 $J_{\text{noise}}$  is the current input.  $J_{\text{pump}}$ ,  $J_{\text{leak}}$  are the calcium fluxes defined
as in [3]..
Output
-----
If the astrocyte receives excitatory synaptic inputs, it might
output SIC to its target neurons. This current depends on the cytosolic
calcium concentration. This dependency is modeled according to the expressions
first proposed in [3]:
.. math:
I_{\text{SIC}} = \mathit{SIC}_{\text{scale}} \cdot \mathit{H}(\ln(y))
where
.. math:
y = \left( \mathit{Ca}^{(2+)} - \mathit{SIC}_{\text{th}} \right) / \mathit{nM}
When the cytosolic calcium concentration of the astrocyte exceeds the threshold
value ( $\mathit{SIC}_{\text{th}}$ ), a SIC output ( $I_{\text{SIC}}$ ) is generated. This thresholding is modeled as a Heaviside function
( $H(\cdot)$ ). In this implementation, the SIC threshold
 $\mathit{SIC}_{\text{th}}$  as well as the scaling constant
```

→
In vivo brain



Potjans and Diesmann (2015)

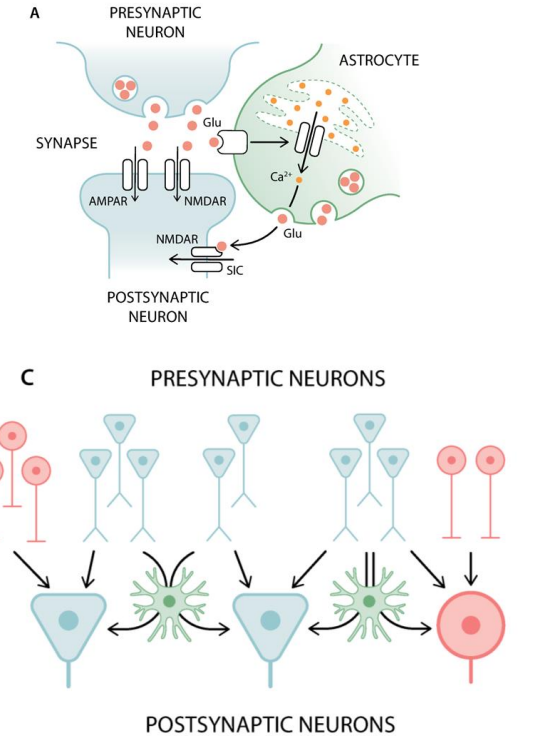
→
**In vitro
cell culture**



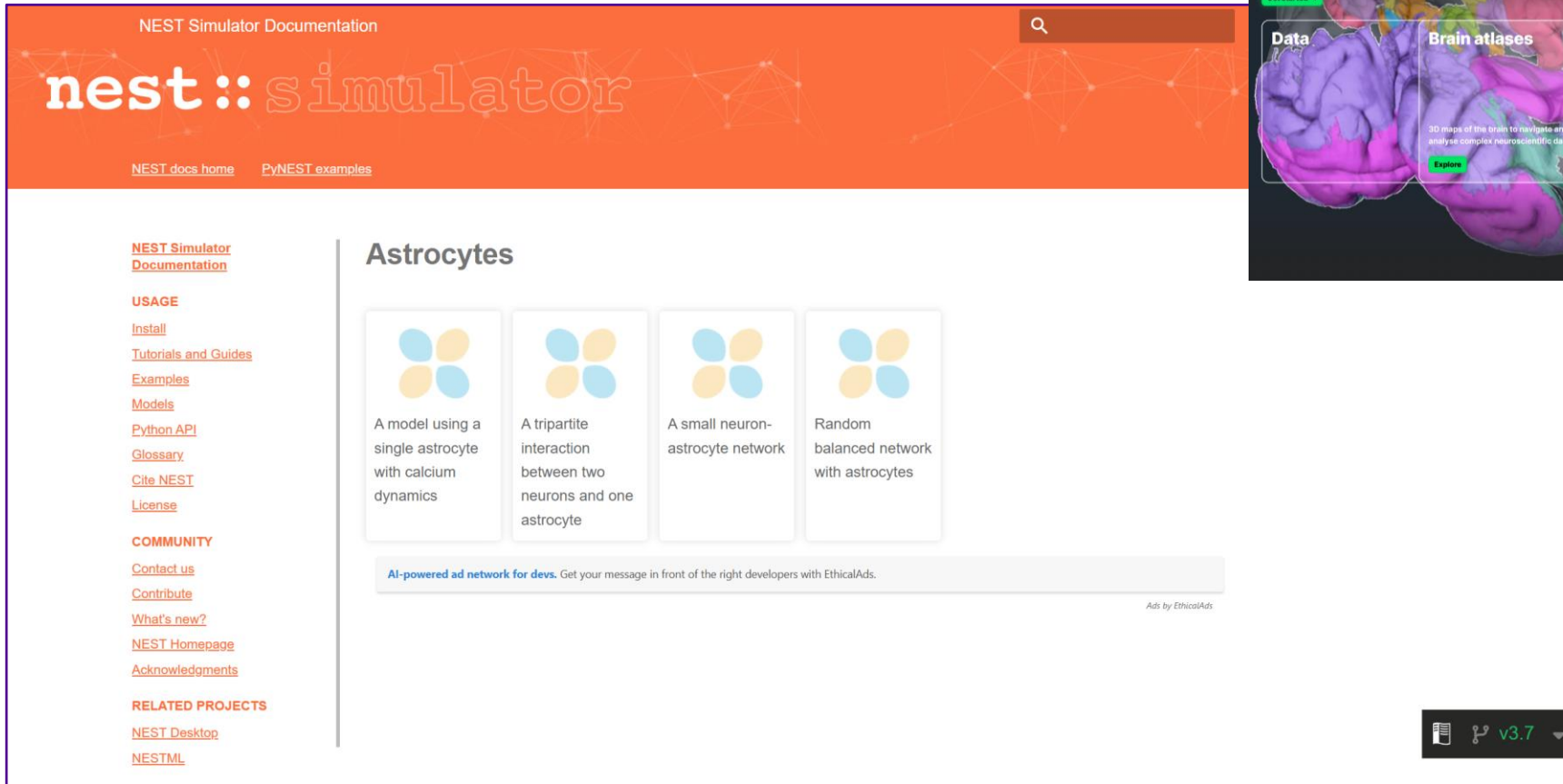
Mäki-Marttunen, Linne et al. (2011, 2013)
Acimovic, Linne et al. (2015)
Teppola, Linne et al. (2019)

Modeling neuron-astrocyte networks: Key achievements

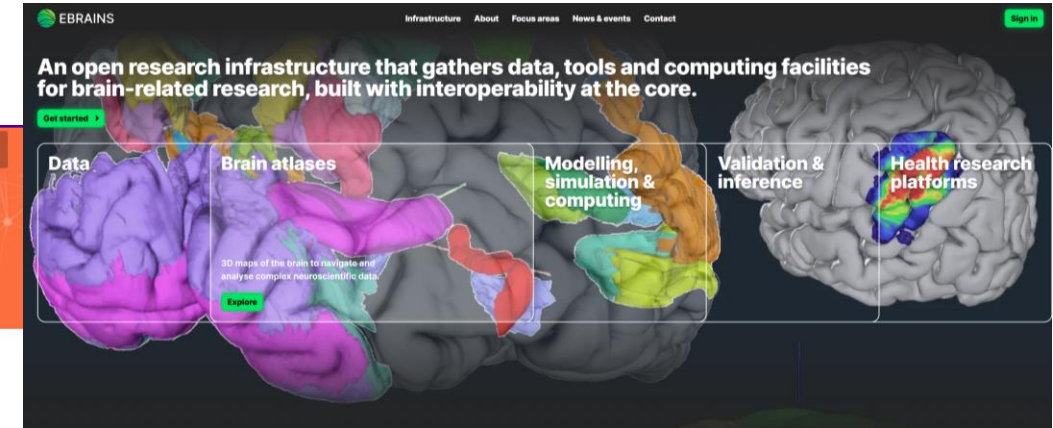
- **Model-building framework** for neuron-astrocyte networks.
- **Connectivity concepts** for tripartite neuron-astrocyte interactions in networks.
- **Scalable architecture** capable of simulating networks with up to a **million cells**.
- Formalized description of neuron-astrocyte modeling facilitates **reproducibility**.
- Integrate **experimental data** to a greater extent than existing studies (Jiang et al. 2025, Manninen et al. 2023)
- Neuron-astrocyte interactions drive the **emergence of synchronization** in local neuronal groups.
- Publicly available in NEST 3.8.



Tutorials



The screenshot shows the NEST Simulator Documentation website. At the top, there's a navigation bar with links for "NEST docs home" and "PyNEST examples". Below the header, the main content area is titled "Astrocytes". It features four small diagrams illustrating different network models involving astrocytes. From left to right: 1. A model using a single astrocyte with calcium dynamics, showing three yellow circles. 2. A tripartite interaction between two neurons and one astrocyte, showing three yellow circles and three blue circles. 3. A small neuron-astrocyte network, showing three yellow circles and three blue circles. 4. Random balanced network with astrocytes, showing four yellow circles and four blue circles. Below these diagrams, there's a note about EthicalAds and a version indicator "v3.7".



EBRAINS:
Digital Brain Infrastructure



<https://github.com/nest/nest-simulator/>

https://nest-simulator.readthedocs.io/en/v3.7/auto_examples/astrocytes/index.html

2.2. Example:

Neuron-astrocyte-vasculature interactions to explain BOLD fMRI signal

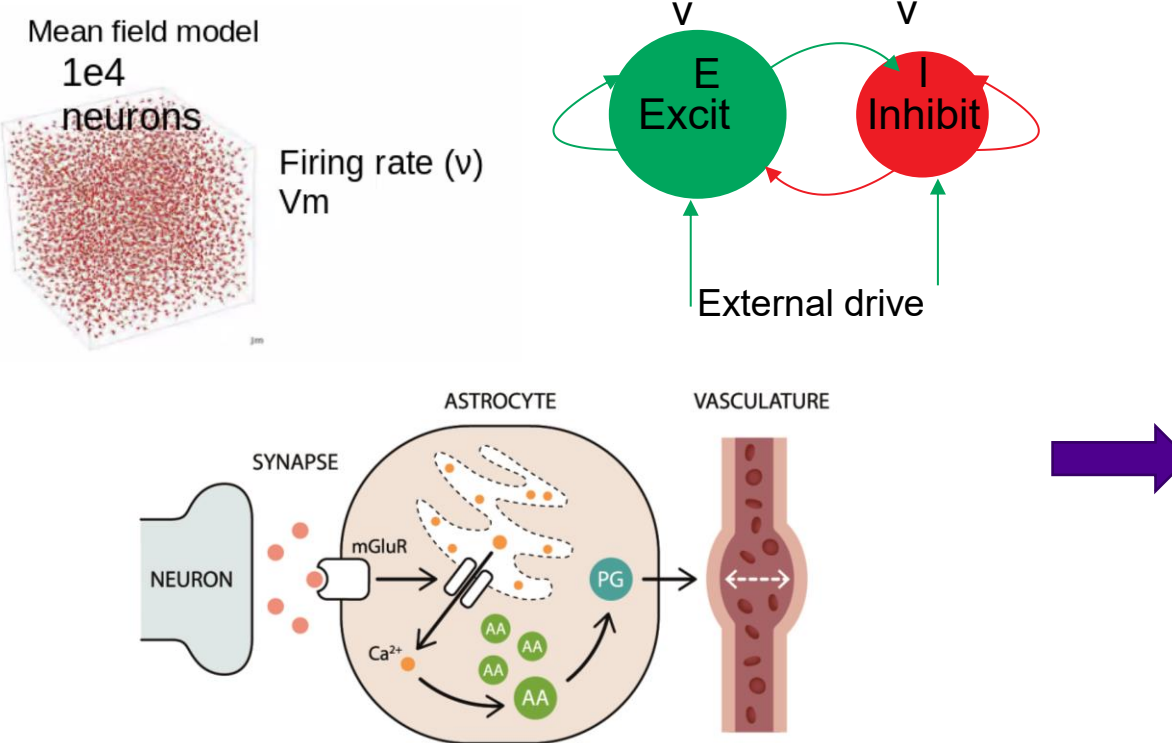
Neuron-astrocyte-vasculature interactions to explain BOLD fMRI signal



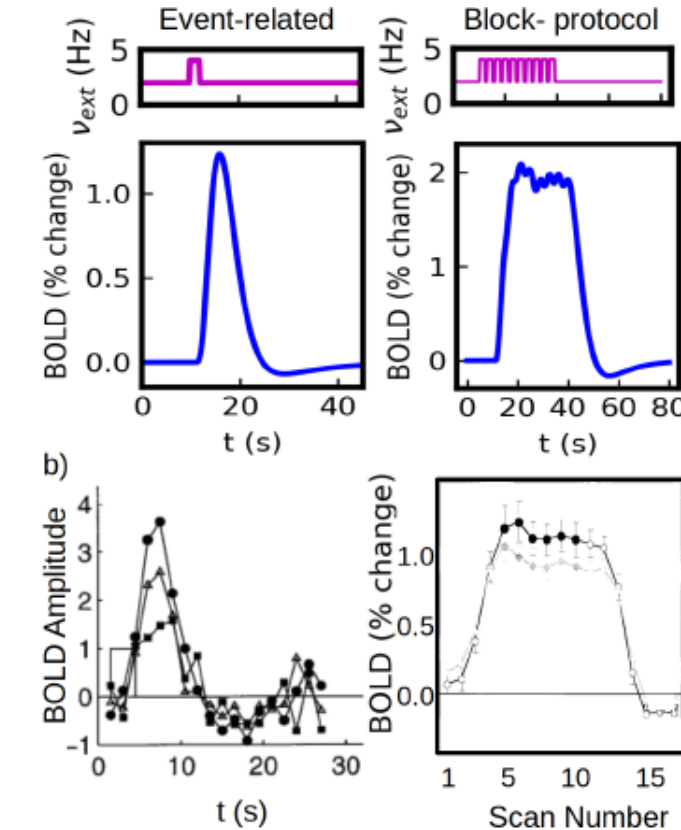
Alain
Destexhe



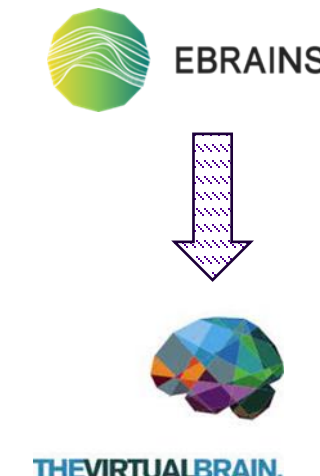
Federico
Tesler



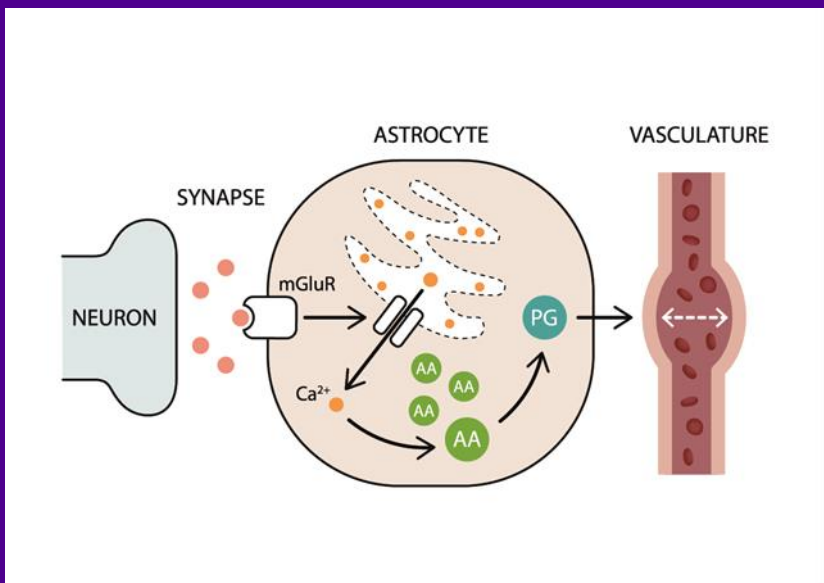
Modeling neuronal, astrocytic and vascular functions underlying BOLD fMRI signal
(point representations)



Tesler, Linne, Destexhe (2023) Scientific Reports



Neuron-synapse-vasculature interactions



www.nature.com/scientificreports/

scientific reports

Check for updates

OPEN

Modeling the relationship between neuronal activity and the BOLD signal: contributions from astrocyte calcium dynamics

Federico Tesler¹*, Marja-Leena Linne² & Alain Destexhe¹

Functional magnetic resonance imaging relies on the coupling between neuronal and vascular activity, but the mechanisms behind this coupling are still under discussion. Recent experimental evidence suggests that calcium signaling may play a significant role in neurovascular coupling. However, it is still controversial where this calcium signal is located (in neurons or elsewhere), how it operates and how relevant is its role. In this paper we introduce a biologically plausible model of the neurovascular coupling and we show that calcium signaling in astrocytes can explain main aspects of the dynamics of the coupling. We find that calcium signaling can explain so-far unrelated features such as the linear and non-linear regimes, the negative vascular response (undershoot) and the emergence of a (calcium-driven) Hemodynamic Response Function. These features are reproduced here for the first time by a single model of the detailed neuronal-astrocyte-vascular pathway. Furthermore, we analyze how information is coded and transmitted from the neuronal to the vascular system and we predict that frequency modulation of astrocytic calcium dynamics plays a key role in this process. Finally, our work provides a framework to link neuronal activity to the BOLD signal, and vice-versa, where neuronal activity can be inferred from the BOLD signal. This opens new ways to link known alterations of astrocytic calcium signaling in neurodegenerative diseases (e.g. Alzheimer's and Parkinson's diseases) with detectable changes in the neurovascular coupling.

Functional magnetic resonance imaging (fMRI) has become one of the leading neuroimaging techniques in neuroscience. fMRI methods rely on the coupling between local neuronal activity and cerebral blood flow (CBF)^{1,2}. In normal conditions an increase in neuronal activity is followed by an increase in CBF, which supplies the necessary oxygen and glucose to sustain the cerebral metabolism, a process known as *functional hyperemia*. In a healthy brain, the increase in oxygen supply overshadows the oxygen demand generating an increase in the local level of blood oxygenation, which is captured by the BOLD (Blood-Oxygen-Level-Dependent) signal³. Although the neurovascular coupling has been extensively demonstrated, the mechanisms behind it remain under discussion. It is currently believed that glutamatergic synapses may play a central role in functional hyperemia^{4,5}, inducing an increase of CBF via two main signaling pathways: a direct neuron-vascular pathway and a neuron-astrocyte-vascular pathway^{6,7}. In both pathways, a glutamate-induced increase in intracellular calcium concentrations (in neurons or astrocytes) triggers the production and release of a variety of vasoconstrictors which generate a dilation of nearby arterioles and an increase in CBF. Among these vasoconstrictors we find potassium (K^+) and hydrogen (H^+) ions, prostaglandins (PGs), epoxyeicosatrienoic acid (EET) and nitric oxide (NO)^{7,8}.

The relative relevance of these different signaling pathways is still under study. In particular, the role of astrocytes in the neurovascular coupling has been in the center of a controversy during the last decade. Some early studies suggested that astrocytic response was too slow to account for functional hyperemia^{9,10}, which raised doubts about the participation of astrocytes in the coupling. However, due to experimental limitations, only somatic responses were measured in these early studies. It was later shown that a fast response can be observed in astrocytic processes and end-feet (from where vasoconstrictors are thought to be released) and can be correlated with the initiation of the vascular response^{11,12}. Thus, while a slow (or null) response may occur at the soma level, a fast response at astrocytic micro-domains is likely associated with the activation of the vascular response. Although further studies are necessary, the role of astrocytes in the neurovascular coupling is increasingly accepted¹³. The actual mechanism behind neurovascular coupling is likely a combination of direct neuron-vascular and

*CNRS, Paris-Saclay Institute of Neuroscience (NeuroPSI), Paris-Saclay University, 91400 Saclay, France. ²Faculty of Medicine and Health Technology, Tampere University, 33720 Tampere, Finland. [✉]email: ftesler@gmail.com

Scientific Reports | (2023) 13:6451 | https://doi.org/10.1038/s41598-023-32618-0

nature portfolio



Alain
Destexhe



Federico
Tesler

Blood Oxygen Level Dependent (BOLD) fMRI

- BOLD fMRI is one key neuroimaging technique used to study human brain activity by detecting changes in **blood oxygenation** linked to **neural activity**.
- While fMRI is a crucial tool in **human neuroscience**, the **exact origins of the BOLD signal** are still not fully understood.

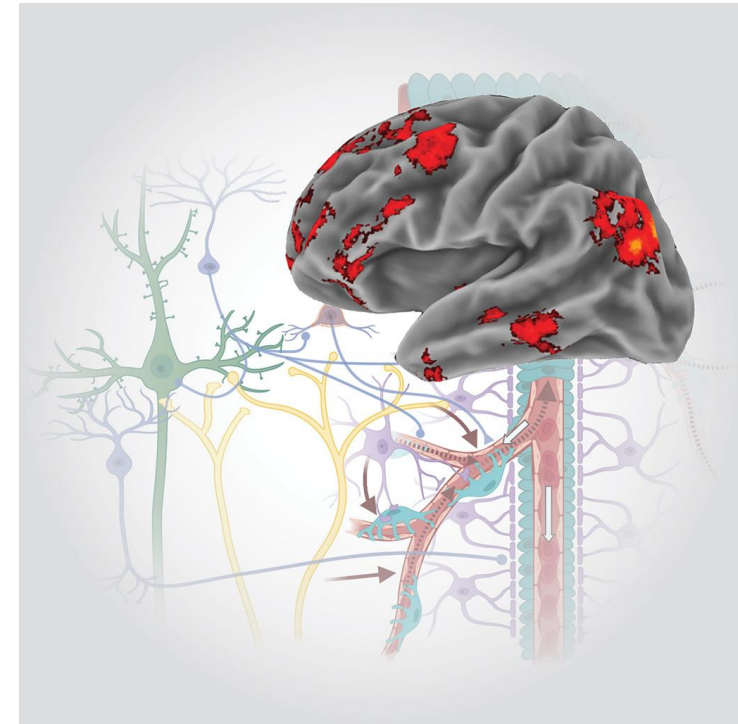
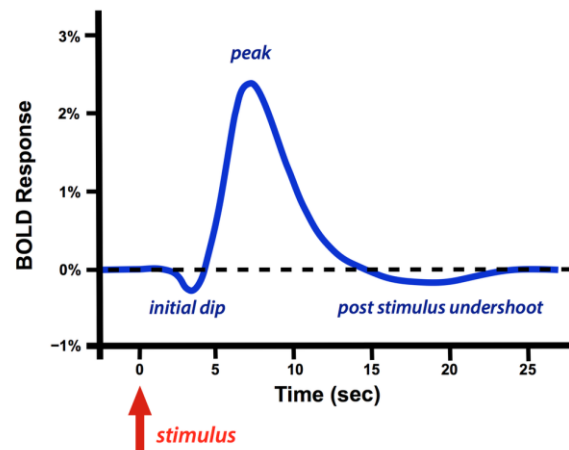
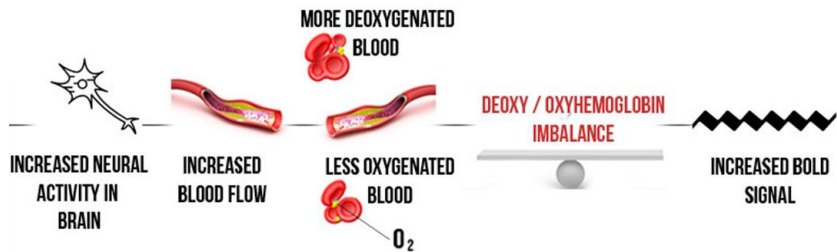
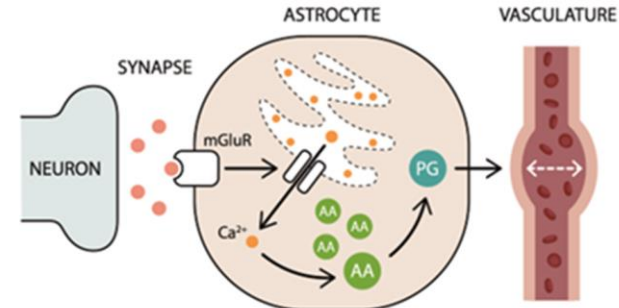
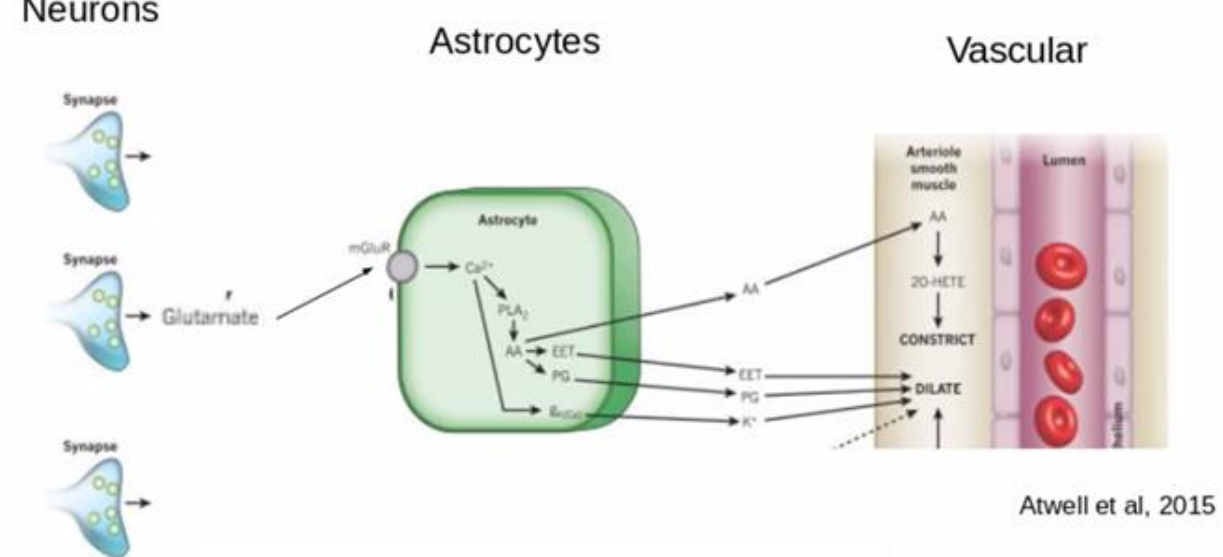


Figure from: Howarth et al., More than just summed neuronal activity: how multiple cell types shape the BOLD response. Philosophical Transactions of the Royal Society B, 2021

Neurons and astrocytes in neurovascular coupling

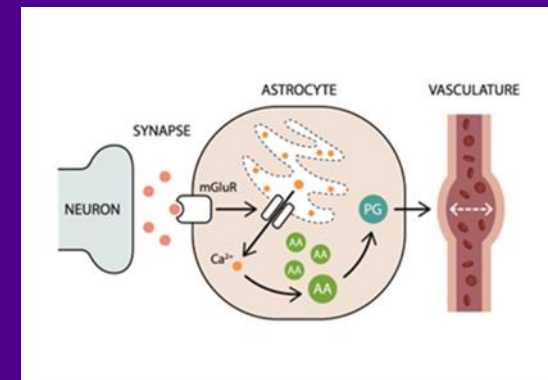
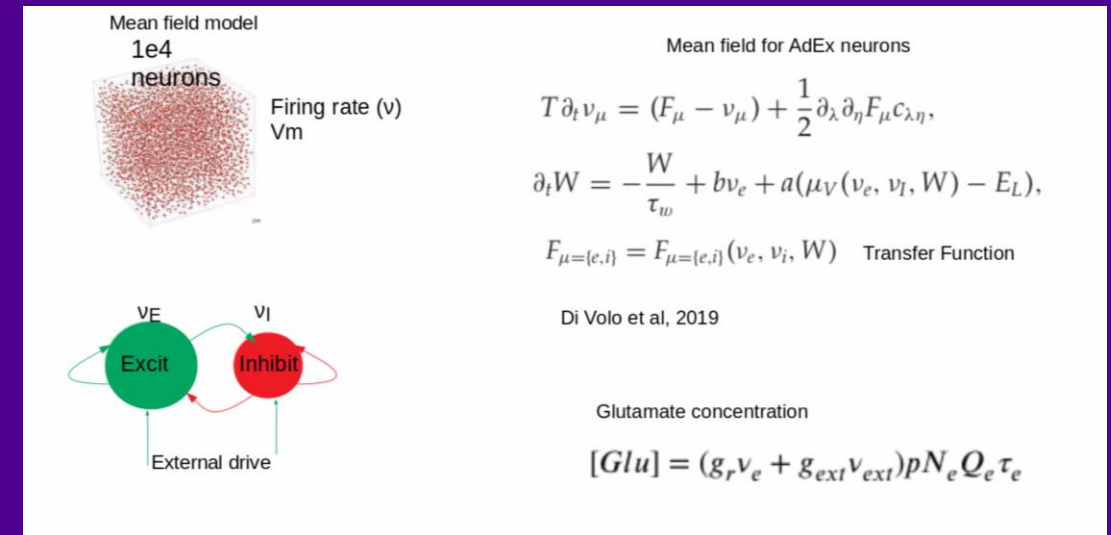
- Neurons release neurotransmitter glutamate.
- Glutamate is detected by postsynaptic cells, but also by astrocytes.
- Our hypothesis (based on Attwell et al. 2015 and others): A complex signaling cascade is induced leading to release of prostaglandins (PG) from astrocytes.
- PG leads to vasodilation in vasculature.



Mathematical model for neuronal components

Population model of neurons:

- Mean-field of AdEx IF:
 - AdEx IF: Adaptive Exponential Integrate-and-Fire neurons
 - Mean-field (from physics): Statistical approximation capturing the collective dynamics of neuronal populations.
- Simplifies the mathematical representation.



Mathematical model for astroglial components

De Pittá et al, 2009:

Astro. Glut. Receptors

$$\tau_A \frac{d}{dt} \gamma_A = -\gamma_A + O_M (1 - \zeta) Y_S (1 - \gamma_A) \tau_A$$

Cytosolic IP3 concentration

$$\frac{d}{dt} I = J_\beta(\gamma_A) + J_\delta(C, I) - J_{3K}(C, I) - J_{5P}(I)$$

$$J_\beta(\gamma_A) = O_\beta \gamma_A, \quad \text{phospholipase C}\beta\text{- and C}\delta\text{-mediated production}$$

$$J_\delta(C, I) = O_\delta \frac{\kappa_\delta}{\kappa_\delta + I} \mathcal{H}(C^2, K_\delta),$$

$$J_{3K}(C) = O_{3K} \mathcal{H}(C^4, K_D) \mathcal{H}(I, K_3)$$

$$J_{5P}(I) = \Omega_{5P} I \quad \begin{matrix} \text{degradation by IP3} \\ \text{3-kinase (3K) and} \\ \text{inositol polyphosphatase 5-phosphatase} \end{matrix}$$

Ca²⁺ dynamics (Li-Rinzel):

$$\frac{d}{dt} C = J_C(C, h, I) + J_L(C) - J_P(C)$$

$$\frac{d}{dt} h = \frac{h_\infty(C, I) - h}{\tau_h(C, I)}$$

$$J_C(C, h, I) = \Omega_C m_\infty^3 h^3 (C_T - (1 + \varrho_A) C),$$

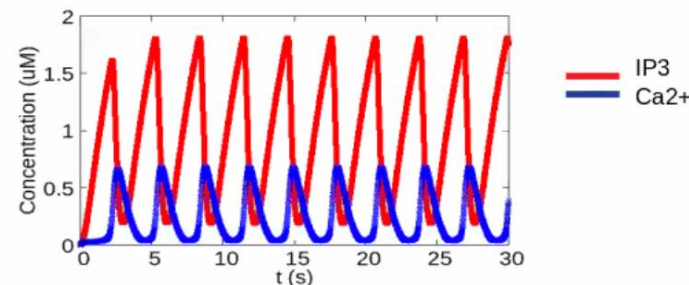
$$m_\infty(C, I) = \mathcal{H}(I, d_1) \mathcal{H}(C, d_5), = \text{IP3*Ca2} / ((\text{IP3+d1})(\text{Ca2+d5}))$$

$$J_L(C) = \Omega_L (C_T - (1 + \varrho_A) C),$$

$$J_P(C) = O_P \mathcal{H}(C^2, K_P),$$

$$h_\infty(C, I) = d_2 \frac{I + d_1}{d_2(I + d_1) + (I + d_3)C},$$

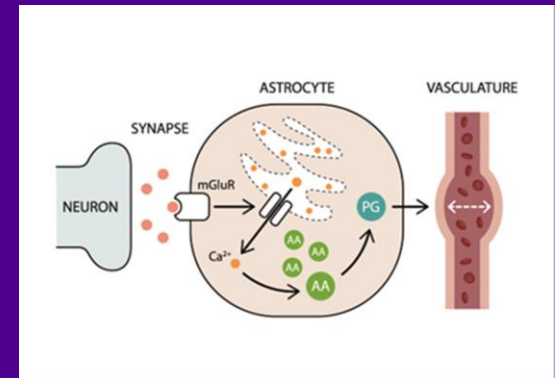
$$\tau_h(C, I) = \frac{I + d_3}{\Omega_2(I + d_1) + O_2(I + d_3)C}.$$



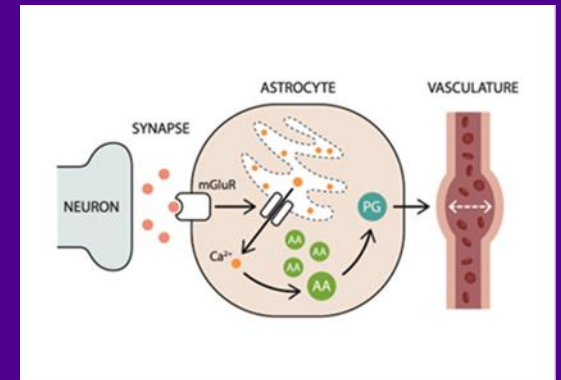
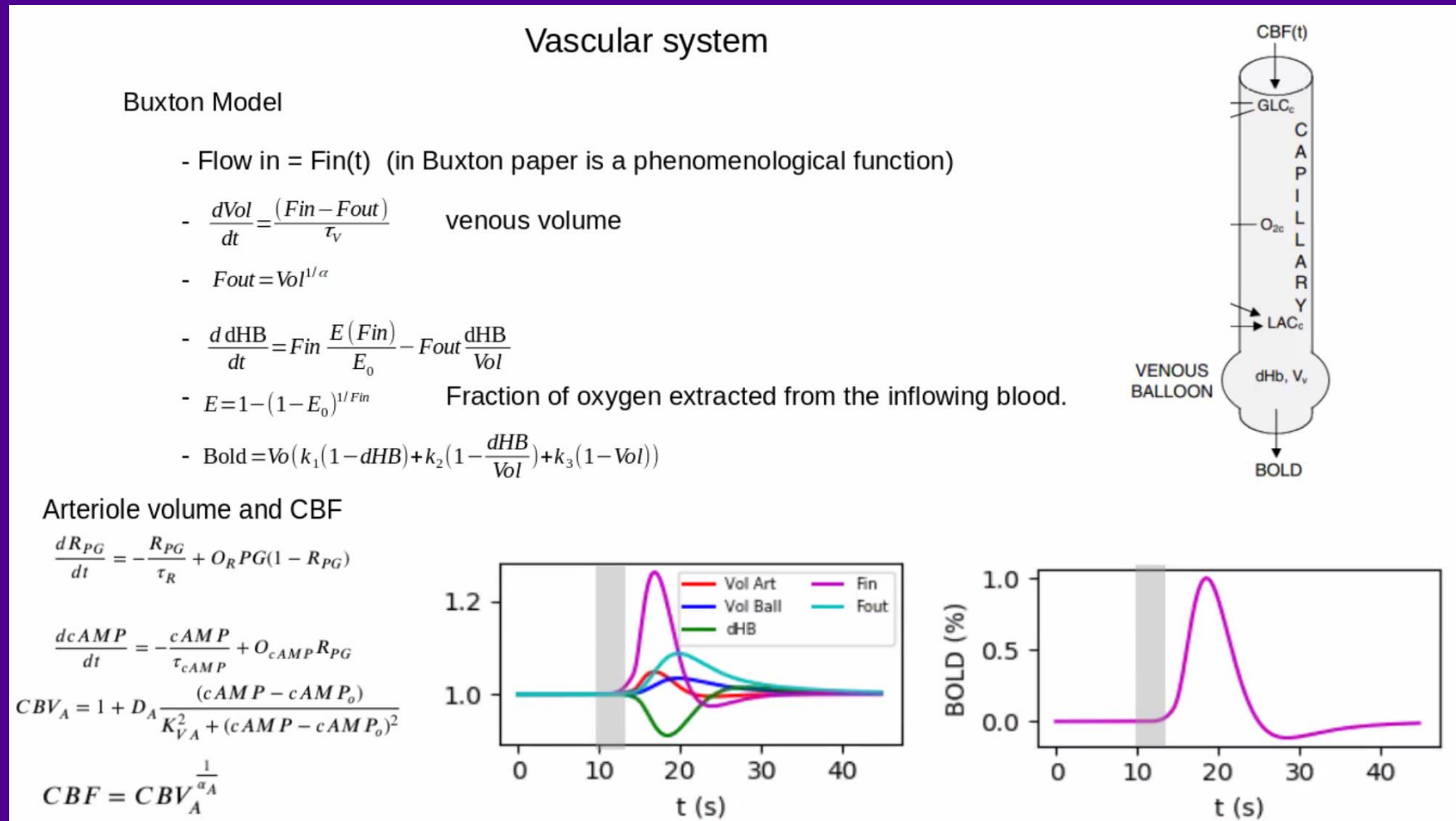
$$\frac{dAA}{dt} = -\frac{AA}{\tau_{AA}} + \frac{O_{AA} Ca^{2+}}{K_{AA} + Ca^{2+}}$$

$$\frac{dPG}{dt} = -\frac{PG}{\tau_{PG}} + \frac{O_{PG} AA}{K_{PG} + AA}$$

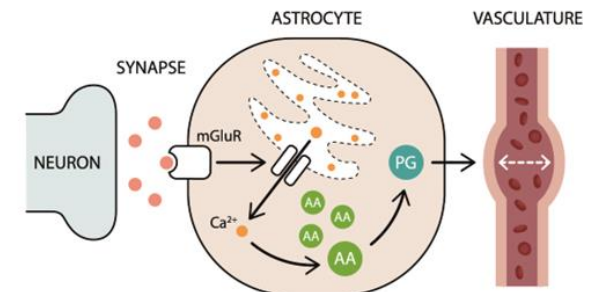
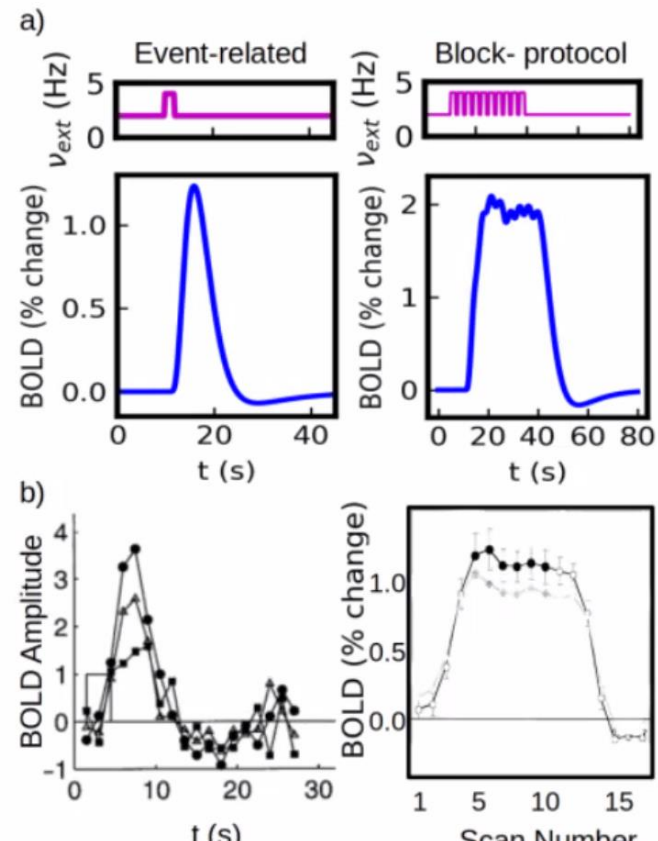
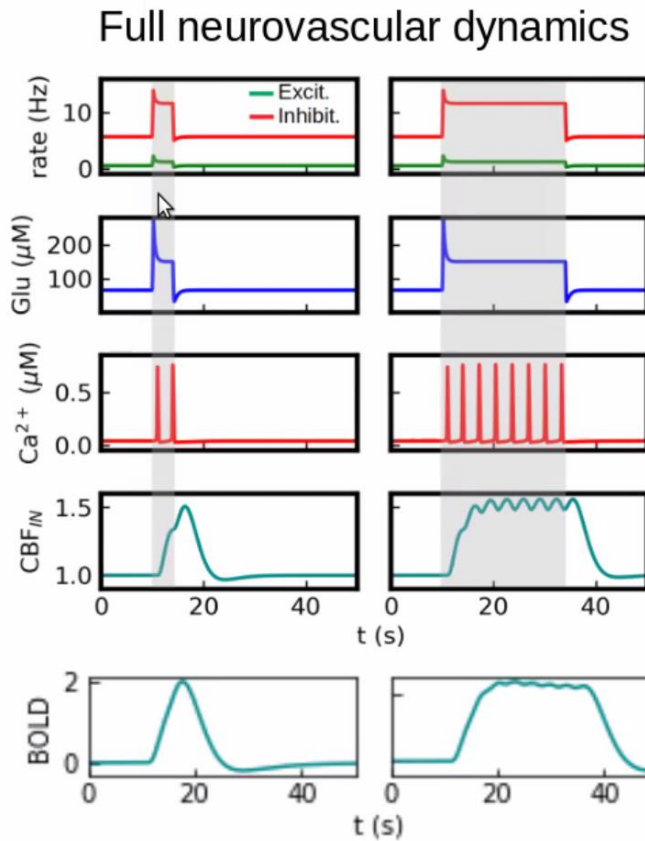
AA and PG production



Mathematical model for vascular components



Model validation



In Silico simulation

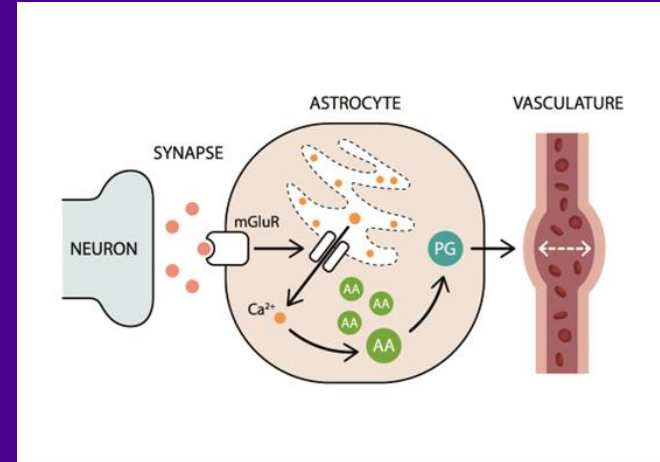
BOLD fMRI imaging

Model predictions

- Calcium signaling, particularly in astrocytes, explains previously unrelated features of the hemodynamic response, such as:
 - Linear and non-linear regimes
 - The negative vascular response (undershoot)
 - The emergence of a **calcium-driven** Hemodynamic Response Function (HRF)
- Frequency modulation of astrocytic calcium dynamics plays a critical role in shaping the HRF, which can be experimentally tested *in vivo*.
- Potential to serve as a **computational biomarker** for understanding brain function, dysfunction, and disease.

Conclusions

- **Biophysically Detailed Modeling:**
 - We have for the first time successfully reproduced HRF features using a **biophysically detailed neuron-astrocyte-vasculature model**.
- **Linked Neural Activity to BOLD Signal:**
 - Our work provides a framework to connect **neuronal and astrocytic activity** to the BOLD signal, allowing for the **inference of brain activity from fMRI data**.
- **New Insights into Neurodegenerative Diseases:**
 - This approach offers new possibilities for linking **altered astrocytic calcium signaling** in neurodegenerative diseases (e.g., Alzheimer's and Parkinson's) to detect changes in **neurovascular coupling**.



3. Summary of tools for astrocyte modeling

Tools for astrocyte modeling

NEURON:

- New specialized tools that can be integrated with NEURON: **ASTRO, ARACHNE**
- Software builders that can be used to create single astrocyte simulations and network simulations (but use with caution!).

NEST:

- Neuron-astrocyte interaction module
- **New tripartite connectivity concept**
- Phenomenological model for astrocytic Ca^{2+} dynamics

Brian2:

- Python scripts
- Phenomenological model for Ca^{2+} dynamics in single astrocytes and networks of astrocytes

Other simulators:

- **STEPS**: Stochastic reaction–diffusion simulator in complex 3D geometries using Gillespie's algorithm on tetrahedral meshes.
- **MCell**: Particle-based Monte Carlo simulator tracking individual molecules' diffusion and reactions in detailed 3D cellular environments.

Summary of all three lectures

- Glial cells have become major players in the functioning of neural circuits.
- Astroglia is actively involved in neurotransmission, cognition, and behavior.
- Astroglial morphologies and calcium signals *in vivo* are urgently needed for modeling.
- Glial models differ from neuron models due to the different properties of glia.
- Modeling neuron-astroglia interactions can solve the contradictory hypotheses in glioscience and explain brain phenomena/signals measured from humans.

Recent publications on astrocyte modeling

- Jiang, J. Aćimović, T. Manninen, I. Ahokainen, J. Stapmanns, M. Lehtimäki, M. Diesmann, S.J. van Albada, H.E. Plessner, **M.-L. Linne**. Modeling neuron-astrocyte interactions in neural networks using distributed simulation. *PLoS Computational Biology* **2025**.
- G. Rabuffo, A. Bandyopadhyay, C. Calabrese, K. Gudibanda, D. Depannemaeker, M.L. Takarabe, M.L. Saggio, M. Desroches, A. Ivanov, **M.-L. Linne**, C. Bernard, S. Petkoski, V.K. Jirsa. Biophysically inspired mean-field model of neuronal populations driven by ion exchange mechanisms. *eLife* **14:RP104249**, **2025**.
- **M.-L. Linne**. Computational modeling of neuron-glia signaling interactions to unravel cellular and neural circuit functioning. *Current Opinion in Neurobiology* **85:102838**, **2024**.
- K. Amunts, **M.-L. Linne** et al. The coming decade of digital brain research: A vision for neuroscience at the intersection of technology and computing. *Imaging Neuroscience* **2:1-35**, **2024**.
- T. Manninen, J. Aćimović, **M.-L. Linne**. Analysis of Network Models with Neuron-Astrocyte Interactions. *Neuroinformatics* **21**, 375–406, **2023**.
- **M.-L. Linne**, J. Aćimović, A. Saudargiene, T. Manninen. Neuron–Glia Interactions and Brain Circuits. In: Giugliano, M., Negrello, M., Linaro, D. (eds) Computational Modelling of the Brain. *Advances in Experimental Medicine and Biology*, vol 1359, **2022**. Springer, Cham.
- O. Eriksson, U.S. Bhalla, K.T. Blackwell, S. Crook, D.X. Keller, A. Kramer, **M.-L. Linne**, A. Saudargienė, R.C. Wade, J. Hellgren Kotaleski. Combining hypothesis- and data-driven neuroscience modeling in FAIR workflows. *eLife* **11:e69013**, **2022**.
- T. Manninen, A. Saudargiene, **M.-L. Linne**. Astrocyte-mediated spike-timing-dependent long-term depression modulates synaptic properties in the developing cortex. *PLoS Comput Biol* **16(11)**: e1008360, **2020**.
- T. Manninen, R. Havela, **M.-L. Linne**. Computational models for calcium-mediated astrocyte functions. *Frontiers in Computational Neuroscience* **12:14**, **2018**.

